NEUROSCIENCE

KIBRA anchoring the action of PKMζ maintains the persistence of memory

Panayiotis Tsokas[1,2]†, Changchi Hsieh[1]†, Rafael E. Flores-Obando[1]†, Matteo Bernabo[3], Andrew Tcherepanov[1], A. Iván Hernández[4], Christian Thomas[5]‡, Peter J. Bergold[1], James E. Cottrell[2], Joachim Kremerskothen[5], Harel Z. Shouval[6], Karim Nader[3], André A. Fenton[1,7,8]*, Todd C. Sacktor[1,2,9]*

How can short-lived molecules selectively maintain the potentiation of activated synapses to sustain long-term memory? Here, we find kidney and brain expressed adaptor protein (KIBRA), a postsynaptic scaffolding protein genetically linked to human memory performance, complexes with protein kinase Mzeta (PKMζ), anchoring the kinase's potentiating action to maintain late-phase long-term potentiation (late-LTP) at activated synapses. Two structurally distinct antagonists of KIBRA-PKMζ dimerization disrupt established late-LTP and long-term spatial memory, yet neither measurably affects basal synaptic transmission. Neither antagonist affects PKMζ-independent LTP or memory that are maintained by compensating PKCs in ζ-knockout mice; thus, both agents require PKMζ for their effect. KIBRA-PKMζ complexes maintain 1-month-old memory despite PKMζ turnover. Therefore, it is not PKMζ alone, nor KIBRA alone, but the continual interaction between the two that maintains late-LTP and long-term memory.

INTRODUCTION

How molecules lasting only hours to days can maintain memory that persists weeks to years is a long-standing fundamental question in neuroscience (*1*, *2*). In 1984, Crick (*1*) proposed that the continual interaction between synaptic proteins maintains the strengthening of synapses in the face of molecular turnover. Such a general mechanism can be constrained by the requirement of most theories of memory that information is stored by the persistent enhancement of only the activated synapses of a neuron (*3*). Long-term potentiation (LTP) is widely considered a putative physiological substrate of memory because strong afferent synaptic stimulation persistently potentiates only activated synaptic pathways; unstimulated pathways remain unchanged (*4*). Thus, the molecular interaction that maintains synaptic enhancement might also continually target the action of potentiating molecules to activated synapses. Progress toward elucidating this mechanism has been slow, however, because the molecules potentiating synaptic transmission during late-LTP and memory maintenance have not been clearly established.

One molecule that persistently potentiates synaptic transmission is the autonomously active protein kinase C (PKC) isoform, protein kinase Mzeta (PKMζ) (*5*–*10*). PKMζ consists of the independent catalytic domain of the atypical isoform PKCζ. Unlike other PKCs, PKMζ lacks an autoinhibitory regulatory domain and is constitutively and thus persistently active without second messenger stimulation (*11*). Instead, the amount of PKMζ determines its activity (*5*, *11*). PKMζ is selectively expressed in neurons from a dedicated PKMζ mRNA, which is transported to dendrites and, under basal conditions, is translationally repressed (*12*–*15*). Strong afferent synaptic stimulation derepresses the PKMζ mRNA (*12*). This derepression up-regulates new PKMζ synthesis and increases the amount of the kinase in neurons (*12*, *16*–*19*), including in dendritic spines and postsynaptic densities (*20*). In late-LTP maintenance recorded in hippocampal slices, the increased steady-state amount of PKMζ persists for hours in CA1 pyramidal cells (*16*, *17*, *19*). In spatial long-term memory maintenance, the increases last for weeks in selective hippocampal neuronal circuits that were transcriptionally active during initial memory formation (*19*). Spatial memory formation also persistently increases PKMζ in extrahippocampal regions involved in spatial information processing such as retrosplenial cortex but not in thalamus (*19*). Likewise, skilled motor learning resulting in long-term procedural memory increases PKMζ for over a month in sensorimotor cortex (*21*). In contrast to all other PKCs, the persistent increases in PKMζ in LTP and long-term spatial memory maintenance correlate with the extent of persistent synaptic potentiation (*11*, *16*, *17*) and memory retention (*18*).

Evidence for PKMζ's causal role in maintenance initially came from ZIP, an inhibitor of the kinase's catalytic site that, unlike inhibitors of any other signaling molecule, disrupted established late-LTP and long-term memory without affecting basal synaptic transmission (*5*, *7*). However, knockout mice lacking PKMζ (*Prkcz*$^{-/-}$ mice; PKMζ-null mice) still express LTP and memory that is reversed by ZIP (*22*, *23*). These mutant mice, however, compensate for the loss of PKMζ by the persistent activation of PKCs that show short-term increases in wild-type mice, including another atypical isoform, PKCι/λ, that is also sensitive to ZIP (*17*). Blocking PKMζ synthesis with short hairpin RNA (shRNA) or antisense oligodeoxynucleotides that selectively

[1]Department of Physiology and Pharmacology, The Robert F. Furchgott Center for Neural and Behavioral Science, State University of New York Downstate Health Sciences University, Brooklyn, NY 11203, USA. [2]Department of Anesthesiology, State University of New York Downstate Health Sciences University, Brooklyn, NY 11203, USA. [3]Department of Psychology, McGill University, Montreal, Quebec H3A 1G1, Canada. [4]Department of Pathology, The Robert F. Furchgott Center for Neural and Behavioral Science, State University of New York Downstate Health Sciences University, Brooklyn, NY 11203, USA. [5]Internal Medicine D (MedD), Department of Molecular Nephrology, University Hospital of Münster, 48149 Münster, Germany. [6]Department of Neurobiology and Anatomy, University of Texas Medical at Houston, Houston, TX 77030, USA. [7]Center for Neural Science, New York University, New York, NY 10003, USA. [8]Neuroscience Institute at NYU Langone Medical Center, New York, NY 10016, USA. [9]Department of Neurology, State University of New York Downstate Health Sciences University, Brooklyn, NY 11203, USA.
*Corresponding author. Email: tsacktor@downstate.edu (T.C.S.); afenton@nyu.edu (A.A.F.)
†These authors contributed equally to this work.
‡Present address: Institute of Neuropathology, University Hospital Münster, 48149 Münster, Germany.

suppress the translation of PKMζ mRNA, but not PKCι/λ mRNA, prevents late-LTP and long-term memory formation in wild-type animals (*17*, *24*, *25*). Thus, PKMζ synthesis is necessary for wild-type late-LTP and long-term memory, and PKMζ action is sufficient to potentiate synaptic transmission (*5*, *6*, *17*, *25*).

LTP induction that increases PKMζ synthesis within a neuron (*19*) results in potentiation exclusively at activated synapses during LTP maintenance (*17*). Likewise, memory training increases PKMζ (*19*) as well as synaptic strength (*26*) in selective dendritic compartments of memory-activated hippocampal neurons for at least a month despite evidence of the kinase's rapid turnover (*27*, *28*). Moreover, viral overexpression of PKMζ within neocortical neurons does not degrade memory, as predicted by saturating potentiation of all synapses (*29*, *30*); instead, it enhances previously established long-term memory, presumably by strengthening a subpopulation of synapses activated during learning (*31*). PKMζ, however, lacks the regulatory domain by which other PKCs translocate to membrane (*11*). Therefore, how PKMζ action persistently targets activated synapses remains unclear but could be through interaction with another molecule.

A clue to such a partner of PKMζ might come from human memory (*32*). Human episodic memory is a highly polygenic trait involving genes linked in networks (*33*), and one important network node encodes a member of the WW and C2 domain–containing protein (WWC) family, the PKMζ-binding, postsynaptic scaffolding protein, kidney and brain expressed adaptor protein (KIBRA, also known as WWC1) (*28*, *32*, *34*, *35*). Human genome-wide studies reveal that alleles of the *KIBRA* gene associate with variation in normal memory performance (*32*, *33*). KIBRA's function in memory might be evolutionarily conserved because overexpression of a dominant-negative KIBRA in cultured neurons of the molluscan model system *Aplysia* disrupts a cellular analog of classical conditioning (*36*, *37*), and knockdown of *KIBRA* gene expression in mice blocks LTP and memory formation (*28*, *38*–*40*). Coexpressing KIBRA with PKMζ in cultured cells stabilizes the kinase and increases its steady-state level by decreasing PKMζ's elimination through the ubiquitin-proteosome pathway (*28*, *36*, *37*). However, an interaction between endogenous KIBRA and PKMζ in neurons has not been observed. We therefore began by asking whether synaptic stimulation facilitates persistent KIBRA-PKMζ interactions in late-LTP maintenance.

RESULTS

KIBRA-PKMζ complexes persistently increase in LTP maintenance

We used in situ proximity ligation assay (PLA) to detect molecular complexes of KIBRA and PKMζ in late-LTP maintenance (Fig. 1 and fig. S1A). In PLA, pairs of antibodies are linked to oligonucleotides, and if the molecules recognized by the antibodies are within 40 nm, the oligonucleotides generate a DNA that is amplified and detected by fluorescent probes (Fig. 1A) (*41*). To establish late-LTP, we prepared mouse hippocampal slices and briefly tetanized Schaffer collateral/commissural fibers in CA3 stratum (st.) radiatum to potentiate field excitatory postsynaptic potential (fEPSP) responses recorded in CA1 st. radiatum for 3 hours (Fig. 1B) (*42*). As control, we recorded low-frequency test responses in an adjacent slice from the same hippocampus for the equivalent time. The strong stimulation facilitates persistent increases in KIBRA-PKMζ complexes in st. radiatum (Fig. 1B), which accumulate in ~1-μm puncta along CA1 pyramidal cell dendrites (Fig. 1C). In contrast, the complexes do not increase in st. lacunosum-moleculare that receive unstimulated synaptic projections, despite high levels of complexes under basal conditions in this dendritic region. The relatively few complexes in CA1 pyramidal cell bodies of st. pyramidale also do not increase.

In parallel with PLA, we examined KIBRA and PKMζ colocalization a second way by measuring the proteins individually by immunocytochemistry (Fig. 2 and fig. S1B). Stimulation persistently increases the amounts and colocalization of KIBRA and PKMζ in st. radiatum (Fig. 2A). The colocalized proteins accumulate in ~1-μm puncta along CA1 pyramidal cell dendrites (Fig. 2B). Comparing immunocytochemistry and PLA in CA1 pyramidal cell bodies, however, reveals

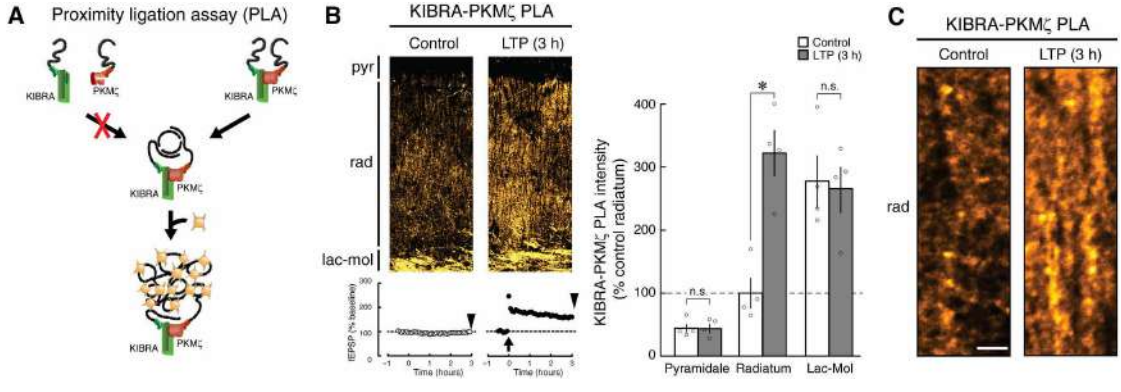

Fig. 1. Strong synaptic stimulation facilitates formation of persistent KIBRA-PKMζ complexes in late-LTP maintenance. (**A**) Schematic of PLA showing KIBRA-PKMζ complexes detected by formation of circular DNA, which is amplified and visualized with a fluorescent probe. (**B**) Persistent increases in KIBRA-PKMζ complexes 3 hours after tetanization in CA1 st. radiatum of mouse hippocampal slice. Top left: representative PLA images reveal complexes increase in st. radiatum (rad) and not in st. pyramidale (pyr) or lacunosum-moleculare (lac-mol), which do not receive stimulated projections. Bottom left: representative test responses and late-LTP, recorded in adjacent slices for 3 hours. Tetanization at arrow; PLA performed at arrowheads. Right: means ± SEM. ANOVA with repeated measurement reveals significant main effect of CA1 sublayers (pyramidale, radiatum, and lacunosum-moleculare, $F_{2,12} = 65.35$, $P < 0.00001$, $\eta^2_p = 0.92$), as well as their interaction ($F_{2,12} = 20.24$, $P = 0.0001$, $\eta^2_p = 0.77$). Post hoc tests show higher PLA intensity in radiatum after LTP, compared to control (*$P < 0.001$), and no significant differences in pyramidale and lacunosum-moleculare ($P = 0.98$ and $P = 0.78$, respectively, n.s., not significant; n's = 4). In untetanized controls, there is no difference between pyramidale and radiatum ($P = 0.18$), whereas lacunosum-moleculare is higher than both pyramidale and radiatum (P's < 0.001). (**C**) Representative images of KIBRA-PKMζ complexes in dendrites within st. radiatum in control and late-LTP maintenance. Scale bar in (C): 50 μm (B) and 5 μm (C).

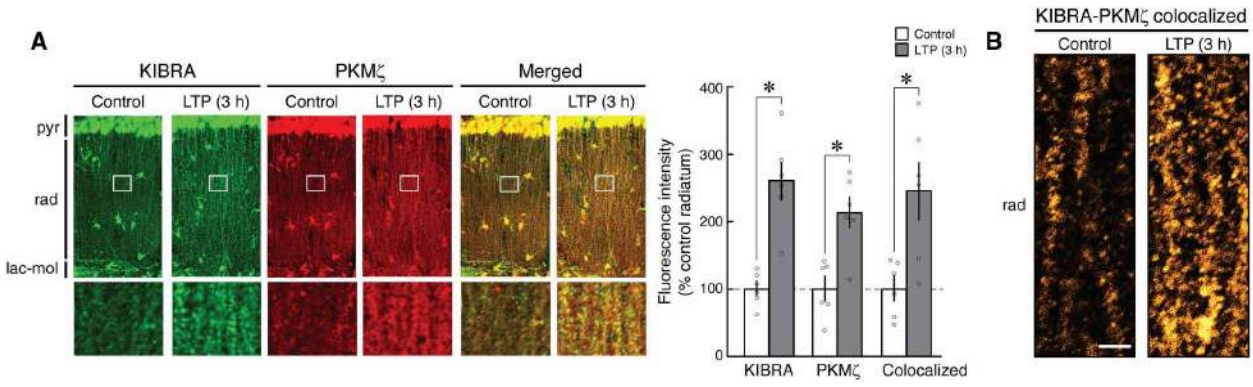

Fig. 2. Strong synaptic stimulation facilitates persistent increases in KIBRA and PKMζ in late-LTP maintenance. (**A**) Left: representative images of total KIBRA (green), total PKMζ (red), and merged signals showing persistent increases in all three in st. radiatum 3 hours after stimulation versus control. Insets below are from areas delineated by gray rectangles above. Right: means ± SEM. Multicomparison *t* tests with Bonferroni correction ($\alpha_{adjusted} = 0.017$ per test) reveal that KIBRA, PKMζ, and their colocalization increase 3 hours after LTP induction compared to control ($t_{10} = 3.97$, $^*P = 0.003$, $d = 2.29$; $t_{10} = 5.42$, $^*P = 0.0003$, $d = 3.13$; and $t_{10} = 3.22$, $^*P = 0.009$, $d = 1.86$, respectively, *n*'s = 6). Comparing the overlap between KIBRA and PKMζ signals in dendritic regions of st. radiatum by Manders coefficients M1 (KIBRA&PKMζ/KIBRA) and M2 (KIBRA&PKMζ/PKMζ) (*83*) indicates that PKMζ is more widely distributed outside areas of colocalization than KIBRA under both control and stimulated conditions. Means ± SEM, M1 (control, 0.57 ± 0.019; stimulated, 0.57 ± 0.024); M2 (control, 0.50 ± 0.025; stimulated, 0.48 ± 0.042). ANOVA with repeated measurement reveals significant main effect of protein, $F_{1,10} = 64.49$, $P < 0.0001$, $\eta^2_p = 0.87$. Post hoc test shows that M1 is higher than M2 under both control and stimulated conditions (*P*'s < 0.001, *n*'s = 6). (**B**) Representative images of colocalized KIBRA and PKMζ (yellow) in puncta and shafts of dendrites in st. radiatum in control and late-LTP maintenance. Scale bar in (B): 50 μm [(A) top], 18 μm [(A) bottom], and 5 μm (B).

high levels of KIBRA and PKMζ yet low levels of KIBRA-PKMζ complexes; therefore, somatic KIBRA and PKMζ do not appear to interact (Figs. 1B and 2A). Thus, strong afferent synaptic activity acts locally within neurons to persistently increase KIBRA-PKMζ interaction.

Blocking the KIBRA-binding site in PKMζ reverses late-LTP maintenance

As most signaling events triggered by strong afferent synaptic activity last for only seconds to minutes (*11*, *43*–*45*), the persistence of KIBRA-PKMζ complexes for hours in late-LTP suggests that sustained KIBRA-PKMζ interaction might maintain late-LTP in wild-type mice. To test this "KIBRA-PKMζ maintenance" hypothesis, we used the small-molecule PKMζ-inhibitor, ζ-stat (1-naphthol-3,6,8-trisulfonic acid), which has been proposed to selectively block the allosteric KIBRA-binding site in the ζ-catalytic domain (Fig. 3A) (*37*). To assess this mechanism of action, we isolated KIBRA-PKMζ heterodimerization/multimerization using the split-Venus bimolecular fluorescence complementation reporter assay (BiFC) (Fig. 3B) (*28*). In this assay, KIBRA and PKMζ fused with complementary fragments of the fluorescent reporter Venus are transfected into human embryonic kidney (HEK) 293T cells, and the interaction of KIBRA and PKMζ produces a fluorescent signal by bringing the two fragments of split-Venus into close apposition (Fig. 3B, left, and fig. S2) (*28*). BiFC reveals that ζ-stat inhibits KIBRA-PKMζ interaction [median inhibitory concentration (IC_{50}) = ~1 μM; Fig. 3B, middle]. In contrast, the ζ-stat at 10 μM has no measurable effect on the interaction of KIBRA with the other atypical isoform, PKCι/λ, which produces BiFC with KIBRA ~10-fold less than PKMζ (Fig. 3B, right). We further validated ζ-stat's mechanism of action by generating a mutant PKMζ[PKCι/λ-P291Q;F297S] with the ζ-stat–binding site in PKMζ changed to the analogous amino acids in PKCι/λ. Interaction of KIBRA with PKMζ[PKCι/λ-P291Q;F297S] is similar to PKCι/λ, and, like PKCι/λ, ζ-stat does not inhibit complexes of mutated PKMζ with KIBRA. ζ-stat also has no effect on KIBRA's interaction with any conventional or novel PKC, the two other classes of PKC isoforms (fig. S3, A and B). Ca^{2+}/calmodulin-dependent protein kinase II alpha (CaMKIIα), another kinase that potentiates synaptic transmission and is important for early-LTP (*44*, *46*), does not measurably interact with KIBRA (fig. S3C).

Now, we can test the central prediction of the KIBRA-PKMζ maintenance hypothesis that decoupling PKMζ from KIBRA reverses potentiation of activated synapses. We simultaneously recorded two independent synaptic pathways in st. radiatum within a hippocampal slice. We stimulated one pathway by high-frequency tetanization to induce late-LTP, and in the second pathway, we recorded low-frequency test fEPSP responses for the equivalent time. After establishing late-LTP for 3 hours, we applied 10 μM ζ-stat to the bath and recorded responses in both pathways for 4 hours (Fig. 4A and fig. S4A). ζ-stat reverses late-LTP maintenance in the stimulated synaptic pathway without measurably affecting synaptic transmission in the control pathway. Thus, ζ-stat disrupts the maintenance of enhanced synaptic transmission selectively at activated synapses, as predicted by the KIBRA-PKMζ maintenance hypothesis.

We tested if the effect of ζ-stat requires PKMζ by examining PKMζ-null mice that recruit compensatory PKMζ-independent mechanisms of late-LTP (*17*). In notable contrast to wild-type mice, ζ-stat has no effect on late-LTP maintenance in mice lacking PKMζ (Fig. 4B and fig. S4A).

If KIBRA-PKMζ coupling in wild-type mice maintains LTP, then, when ζ-stat is washed out, the reversal of potentiation should persist. If another mechanism maintains LTP and KIBRA-PKMζ coupling is a transient, downstream signaling pathway that expresses synaptic potentiation, then, when the drug is washed out, potentiation should return. To distinguish between the KIBRA-PKMζ maintenance hypothesis and this alternative KIBRA-PKMζ downstream-expression hypothesis, after establishing wild-type late-LTP, we applied ζ-stat for 3 hours and then washed the drug out for an additional 4 hours. The reversal of potentiation persisted (Fig. 5A and fig. S4B). To examine if the washout was effective, in separate experiments, we applied the drug for the same 3-hour duration, suppressing late-LTP in one synaptic pathway, and then initiated the washout (Fig. 5B and fig. S4C).

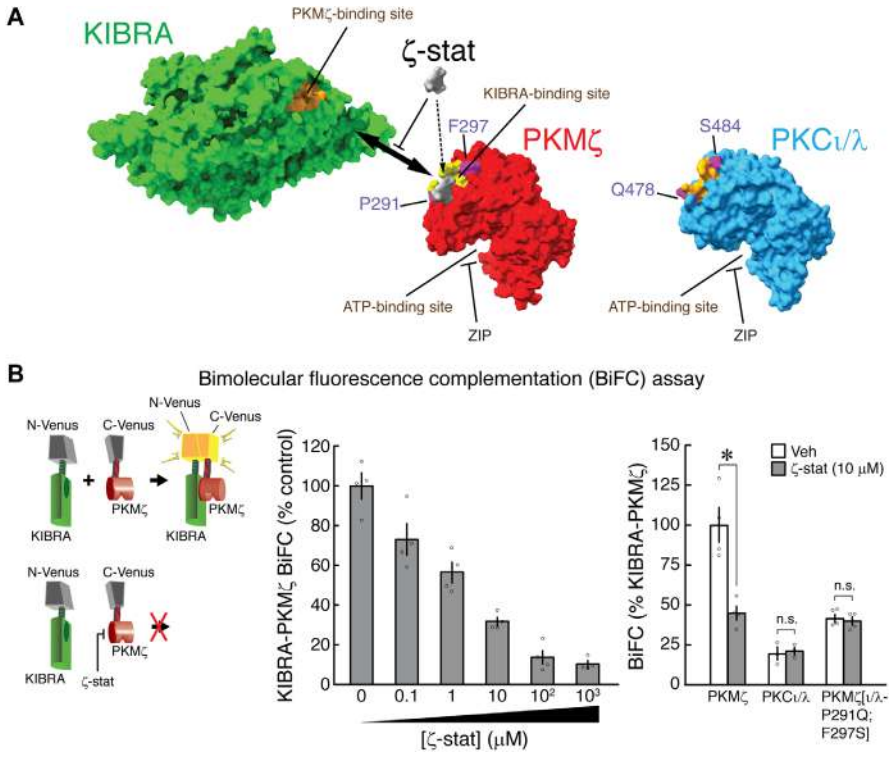

Fig. 3. Inhibitor of the allosteric KIBRA-binding site in PKMζ blocks KIBRA-PKMζ interaction. (**A**) Predicted structures of KIBRA (green) and PKMζ (red) show ζ-stat (gray) interacting with an allosteric pocket in PKMζ within the KIBRA-binding site (yellow). The KIBRA-binding site is flanked by ζ-specific residues P291 and F297 [purple; amino acid numbering based on PKMζ sequence (*12*)]. The KIBRA-binding site in PKMζ is distinct from the ATP-binding and protein-substrate–binding sites, which are also present in the catalytic domain of PKCι/λ (blue) and are inhibited by ZIP. The PKMζ-binding site in KIBRA is shown in orange. (**B**) BiFC shows that ζ-stat inhibits dimerization of KIBRA and PKMζ. Top left: schematic of BiFC reaction showing that dimerization of KIBRA and PKMζ reconstitutes fluorescence reporter split-Venus; bottom left: suppression of BiFC by ζ-stat. Middle: dose-response curve shows ζ-stat IC_{50} of ~1 μM; means ± SEM, *n*'s = 4. Right: ζ-stat (10 μM) inhibits KIBRA interaction with PKMζ but not with PKCι/λ or PKMζ[PKCι/λ-P291Q;F297S], in which the ζ-stat–binding site is changed to the amino acids in PKCι/λ. Means ± SEM; $n = 4$ sets of transfected HEK293T cultures. The two-way ANOVA reveals the main effects of drug (ζ-stat and vehicle, $F_{1,16} = 15.32$, $P < 0.01$, $\eta^2_p = 0.49$) and kinase (PKMζ, PKCι/λ, and mutated PKMζ, $F_{2,16} = 39.42$, $P < 0.000001$, $\eta^2_p = 0.83$) and their interaction ($F_{2,16} = 15.23$, $P < 0.0005$, $\eta^2_p = 0.66$). Post hoc analysis shows that KIBRA binds PKMζ stronger than either mutated PKMζ or PKCι/λ ($P < 0.0002$), whereas binding to mutated PKMζ and PKCι/λ are not significantly different ($P = 0.06$). ζ-stat suppresses KIBRA-PKMζ coupling (*$P < 0.0005$) but has no effects on KIBRA-PKCι/λ and KIBRA-mutated PKMζ ($P = 0.86$ and $P = 0.76$, respectively; n.s.).

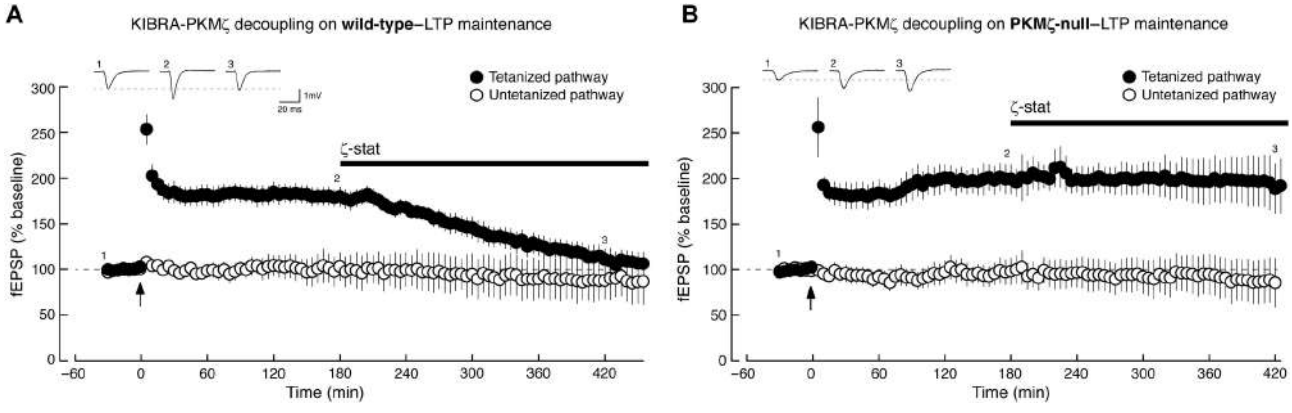

Fig. 4. Inhibitor of the KIBRA-binding site in PKMζ reverses established late-LTP in wild-type mice but not in compensated PKMζ-null mice. (**A**) In hippocampal slices prepared from wild-type mice, ζ-stat (10 μM) applied to the bath 3 hours after tetanization reverses late-LTP as measured by fEPSP slope, with no effect on baseline synaptic transmission recorded in an independent synaptic pathway within the slices. Tetanization is at arrow. Top: numbered representative fEPSP traces correspond to time points noted below. Wild-type tetanized pathways: mean response 5 min before ζ-stat compared to 4 hours after initiation of ζ-stat, $t_6 = 5.41$, $P < 0.01$, $d = 2.46$, $n = 6$; nontetanized pathway: 5 min before ζ-stat versus 4 hours after ζ-stat, $t_3 = 2.30$, $P = 0.43$; $d = 0.49$, $n = 4$. (**B**) In PKMζ-knockout mice (PKMζ-null), ζ-stat (10 μM) applied to the bath 3 hours after tetanization has no effect on late-LTP or baseline synaptic transmission. PKMζ-null tetanized pathways: 5 min before ζ-stat versus 4 hours after ζ-stat, $t_3 = 0.79$, $P = 0.49$, $d = 0.23$, $n = 4$; nontetanized pathways: $t_3 = 0.82$, $P = 0.47$, $d = 0.29$, $n = 4$. Wild-type compared to PKMζ-null at 4 hours after ζ-stat: $t_8 = 2.97$, $P < 0.02$, $d = 1.78$.

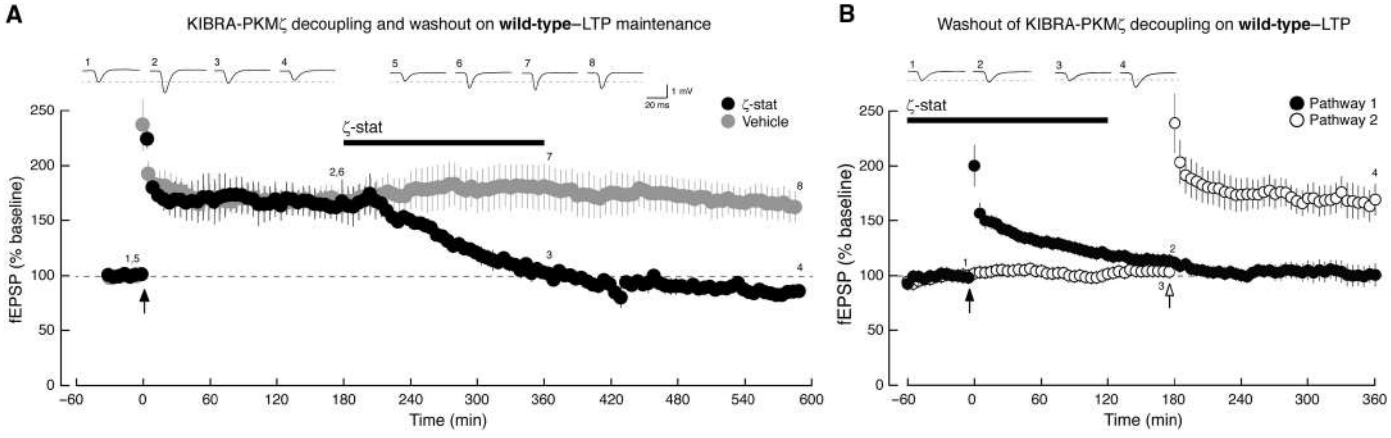

Fig. 5. Inhibitor of the KIBRA-binding site in PKMζ reverses late-LTP, and after drug washout, synaptic potentiation does not return. (**A**) ζ-stat applied 3 hours after tetanization reverses wild-type–LTP maintenance; after 4-hour washout, potentiation does not return (black circles). Two-way ANOVA with repeated measurement shows effects of treatment (ζ-stat and vehicle, $F_{1,7} = 5.95$, $P < 0.05$, $\eta^2_p = 0.46$), time (5 min before tetanization and 180, 360, and 500 min after tetanization, $F_{3,21} = 12.78$, $P < 0.0001$, $\eta^2_p = 0.65$), and interaction ($F_{3,21} = 9.14$, $P < 0.0005$, $\eta^2_p = 0.57$). Post hoc analysis reveals that ζ-stat disrupts LTP (5-min response before tetanization versus 5-min before ζ-stat, $P < 0.005$; 5 min before versus 5 min at end of 3-hour ζ-stat application, $P < 0.005$); the effect persists after washout (5-min period at end of 3-hour application versus 5 min 140 min afterward, $P = 0.2$, $n = 3$). LTP in vehicle is stable (gray circles; before tetanization versus the three time points after tetanization, P's < 0.002, $n = 6$). (**B**) ζ-stat suppresses late-LTP in one pathway, and after 1-hour washout, late-LTP is induced and maintained in the second pathway, indicating effective washout. ANOVA with repeated measurement reveals main effects of treatment (pathways 1 versus 2) and time (5 min before tetanization versus 150 min after tetanization) ($F_{1,8} = 11.46$, $P < 0.01$, $\eta^2_p = 0.59$ and $F_{1,8} = 80.70$, $P < 0.0001$, $\eta^2_p = 0.91$, respectively) and interaction ($F_{1,8} = 29.57$, $P < 0.001$, $\eta^2_p = 0.79$). Post hoc analysis reveals that ζ-stat suppresses late-LTP (5 min before tetanization versus 150 min after tetanization with drug, $P = 0.08$), but after 1-hour washout, late-LTP is induced and maintained in the second pathway (5 min before tetanization versus 150 min after tetanization without drug, $P < 0.0005$). After tetanization responses with and without drug differ, $P < 0.0005$; n's = 5.

After only 1 hour of washout, we stimulated a second synaptic pathway and produced late-LTP, indicating effective drug washout. These results are predicted by the KIBRA-PKMζ maintenance hypothesis and not by the KIBRA-PKMζ downstream-expression hypothesis.

Blocking the KIBRA-binding site in PKMζ disrupts established long-term memory

We next tested the predictions of the KIBRA-PKMζ maintenance hypothesis in active place avoidance, a hippocampus-dependent spatial long-term memory task (Fig. 6). We rapidly conditioned wild-type mice to actively avoid a shock zone by three 30-min training sessions with 2-hour intertrain intervals and then, 1 day later, injected ζ-stat or vehicle bilaterally in hippocampus. Two days after the injection, we tested long-term memory retention with the shock off. Mice that had received vehicle remember to avoid, whereas mice that had received ζ-stat show persistent loss of retention for the shock zone location. In contrast, PKMζ-null mice receiving ζ-stat avoided the shock zone as well as those that had received vehicle, thus controlling for off-target effects of the drug in memory maintenance.

We examined if ζ-stat disrupts maintenance as opposed to other aspects of memory (fig. S5A). Repeating the experiments in wild-type mice, we measured the persistent loss of long-term memory retention without shock and then immediately retrained the mice to avoid another shock zone defined by the cues of a novel context. The mice that had previously been injected with ζ-stat do not remember the location of the first shock zone that was established before the injection, but they learn to avoid and remember a new second location as well as the mice that had received only vehicle. The mice that had earlier received ζ-stat have learning curves in the second context indistinguishable from vehicle-treated mice, demonstrating that ζ-stat does not suppress expression of the avoidance behavior (fig. S5B). Thus, ζ-stat persistently disrupts previously acquired information but, once eliminated, does not impair formation, maintenance, or expression of newly acquired spatial information.

We also examined the consequences of KIBRA-PKMζ decoupling on auditory-cued fear/threat memory maintenance in the basolateral amygdala (BLA) of wild-type and PKMζ-null mice (Fig. 7). One day after conditioning, both wild-type and PKMζ-null mice show increased freezing to tone, confirming previous findings in PKMζ-null mice (*23*). Then, 1 day after the first memory retention testing, the mice were injected with ζ-stat or vehicle bilaterally in BLA and retested the following day. The results reveal that ζ-stat impairs memory retention in wild-type mice and not in PKMζ-null mice. We note that the ζ-stat treatment in wild-type mice results in freezing that is indistinguishable from freezing before presentation of the conditioned stimulus [for analysis of variance (ANOVA), see Fig. 7 legend; post hoc analysis shows $P = 0.34$].

As PKMζ-null mice show a form of PKMζ-independent memory maintenance, we asked if wild-type mice might as well. Previous results with the first-generation PKMζ-inhibitor ZIP revealed that, whereas the agent disrupts cued fear/threat memory, ZIP in hippocampus does not affect contextual fear/threat memory (*47*, *48*). We found that, like ZIP, ζ-stat has no effect on contextual fear/threat memory in hippocampus, in either wild-type mice or PKMζ-null mice (fig. S6). Therefore, wild-type mice store information by both PKMζ-dependent mechanisms and, like PKMζ-null mice, PKMζ-independent mechanisms.

Peptide mimicking the PKMζ-anchoring site in KIBRA reverses late-LTP maintenance and disrupts long-term memory

To further test that blocking KIBRA-PKMζ interaction is an effective way to reverse LTP and memory, we inhibited KIBRA-PKMζ

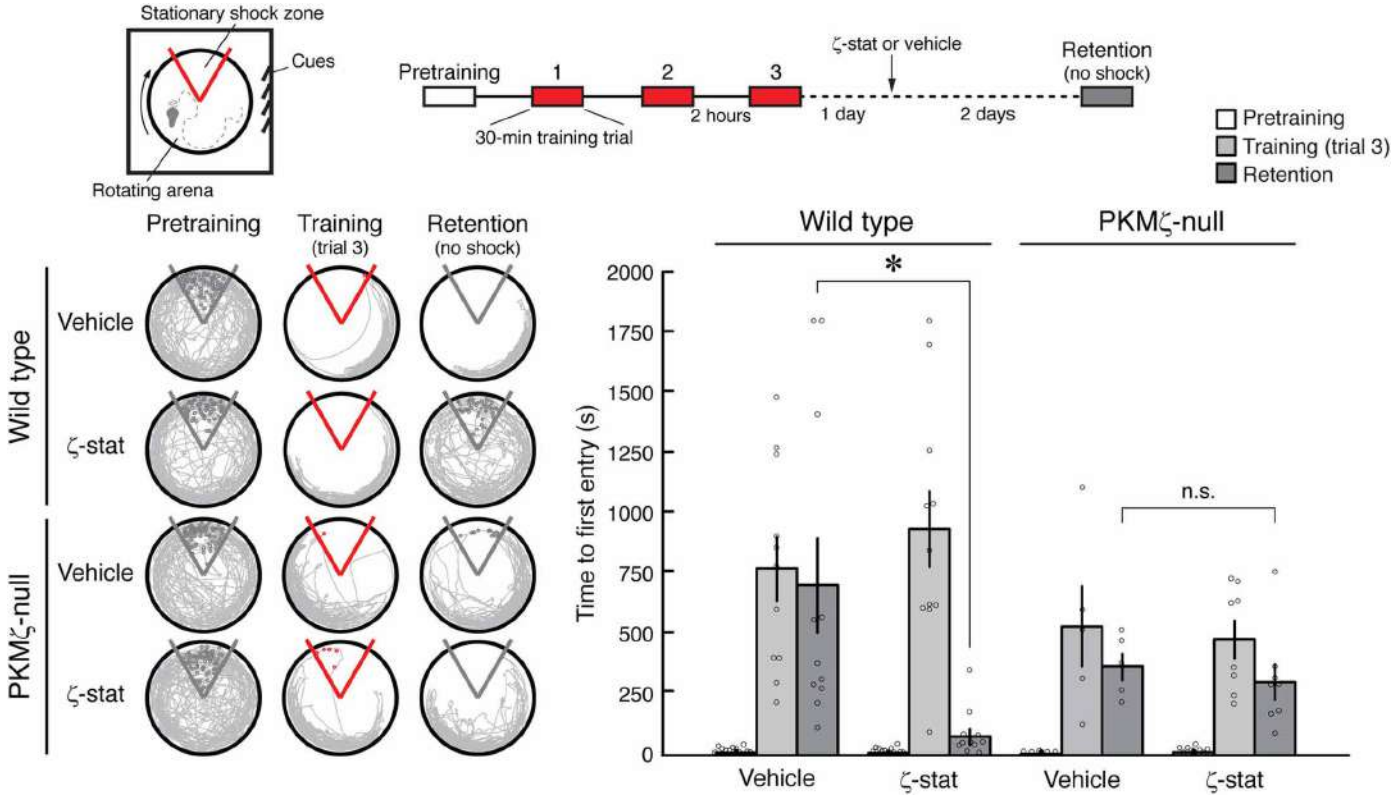

Fig. 6. Inhibitor of the KIBRA-binding site in PKMζ disrupts long-term spatial memory in wild-type mice but not in compensated PKMζ-null mice. (**Top left**) Schematic of place avoidance training apparatus shows slowly rotating arena within which is a nonrotating 60° sector shock zone (delineated in red). Visual cues are on room walls. (**Top right**) Conditioning protocol. Two hours after a 30-min pretraining session without shock, conditioning consists of three trials of 30 min with 2-hour intertrial intervals, producing long-term memory to avoid the shock zone. One day after conditioning, ζ-stat (5 nmol in 0.5-μl vehicle) or vehicle is injected in each hippocampus. Two days after injection, memory retention is tested with shock off, measured as the time to first enter the shock zone. (**Bottom**) ζ-stat disrupts spatial memory retention in wild-type mice but not in PKMζ-null mice. (**Bottom left**) Representative paths during pretraining, the trial at the end of training, and during retention testing with the shock off 3 days after training. Shock zone is shown red with shock on and gray with shock off. Red circles denote where shocks occur; gray circles denote where shocks would have been received if the shock were on. (**Bottom right**) Time to first entry measure of active place avoidance memory (means ± SEM). There is training effect ($F_{2,62} = 37.20$, $P < 0.0001$, $\eta^2_p = 0.55$) and interaction among effects of training, genotype, and treatment (vehicle and ζ-stat) (training x treatment: $F_{2,62} = 3.91$, $P < 0.05$, $\eta^2_p = 0.11$; training x genotype x treatment: $F_{2,62} = 3.29$, $P < 0.05$, $\eta^2_p = 0.096$). Retention in wild-type mice with ζ-stat is different from vehicle (*$P < 0.005$). Retention in PKMζ-null mice with ζ-stat is not different compared with vehicle (n.s.; $P = 0.70$). Wild-types: *n*'s = 11; PKMζ-nulls: vehicle, $n = 5$; ζ-stat, $n = 8$.

dimerization using a cell-permeable, myristoylated peptide that mimics KIBRA's PKMζ-anchoring sequence [myr-N-FVRNSLERRSVRMKRPS-C, KIBRA-based zeta antagonist peptide (K-ZAP); Fig. 8, A and B] (*28*). K-ZAP applied 3 hours after tetanization reverses late-LTP maintenance in wild-type mice, with no measurable effect on baseline synaptic transmission (Fig. 8C and fig. S7). Like ζ-stat, K-ZAP has no effect on late-LTP maintenance in PKMζ-null mice. Intrahippocampal injection of K-ZAP 1 day after active place avoidance conditioning disrupts established spatial long-term memory retention assayed 2 days after injection in wild-type mice (Fig. 9A). K-ZAP has no effect on memory retention in PKMζ-null mice.

Persistent KIBRA-PKMζ coupling maintains remote memory

We examined if KIBRA-PKMζ interaction maintains memory despite PKMζ turnover. PKMζ turns over within a few hours in cultured hippocampal neurons (*27*) and within days in hippocampus in vivo, as indicated by the loss of PKMζ protein after shRNA knockdown of PKMζ mRNA in wild-type animals (*24*, *25*) or inducible deletion of the PKMζ gene in *Prkcz*$^{fl/fl}$ mice (fig. S8). Although PKMζ molecules are replaced, active place avoidance conditioning of wild-type mice produces a stable persistent increase in the steady-state level of PKMζ in hippocampus that lasts for over 4 weeks, and the conditioned behavior remains hippocampus-dependent in the face of systems consolidation (*7*, *19*). We therefore trained mice on active place avoidance and, 4 weeks later, injected either K-ZAP or vehicle bilaterally in hippocampus (Fig. 9B). Retention testing 2 days after injection reveals K-ZAP disrupts remote spatial memory.

DISCUSSION

Previous efforts to understand how molecules store long-term memory focused on the individual actions of single molecules (*9*), such as the persistently active kinases CaMKII and PKMζ that potentiate synaptic transmission (*10*, *46*), or the prion-like properties of translation factors that might perpetuate protein synthesis (*49*). Other investigators have searched for synaptic or extrasynaptic proteins that are especially long-lived (*50*, *51*). Here, building upon a suggestion of Crick (*1*) that persistent molecular interactions sustain memory, we tested the hypothesis that the continual coupling between an autonomously

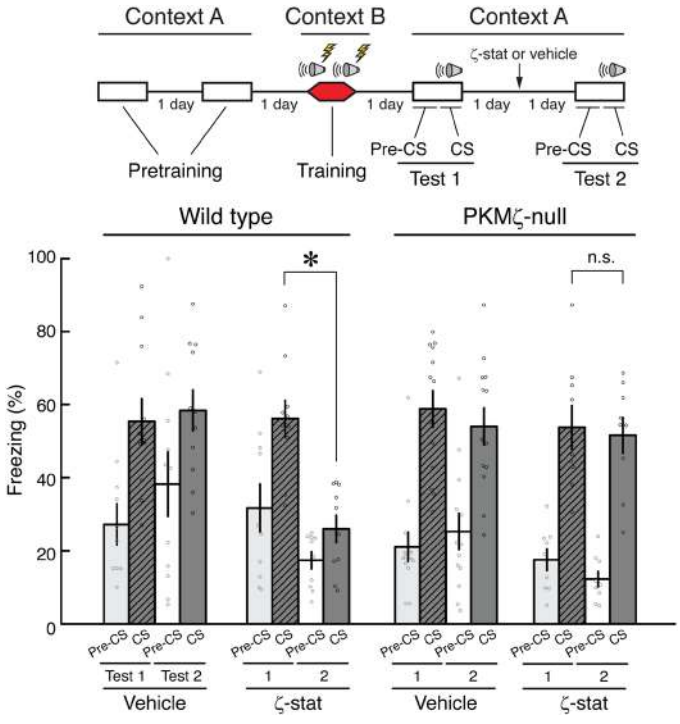

Fig. 7. Inhibitor of the KIBRA-binding site in PKMζ disrupts long-term retention of fear/threat memory in wild-type mice but not in compensated PKMζ-null mice. ζ-stat in BLA disrupts established auditory-cued fear/threat memory. (**Top**) Protocol shows that wild-type and PKMζ-null mice undergo auditory-cued fear/threat conditioning and then retention testing 1 day after training with the conditioned stimulus (CS) tone in a different context from that during conditioning (test 1). The next day, mice receive ζ-stat (6 nmol in 0.3 μl) or vehicle into each BLA and then are tested 1 day after injection (test 2). The freezing responses of two phases (pre-tone and post-tone) within a retention trial are examined. (**Bottom**) ζ-stat disrupts fear/threat memory retention in wild-type mice but not in PKMζ-null mice (means ± SEM of % time freezing). The four-way repeated measures ANOVA (genotype x treatment x trial x phase) reveals that the main effects of treatment, trial, and phase are all significant ($F_{1,39}$'s > 4.79, P's < 0.05, η^2_p > 0.11), as are the interactions of trial x phase, trial x treatment, genotype x phase, and genotype x treatment x trial ($F_{1,39}$'s > 5.26, P's < 0.05, η^2_p > 0.12). Post hoc analysis shows that ζ-stat disrupts the freezing response to CS in the postinjection retention test compared to the preinjection retention test in wild-type mice (*P < 0.0001) but not in PKMζ-null mice (P = 0.64); wild-types: vehicle, n = 11; ζ-stat, n = 10; PKMζ-nulls: vehicle, n = 13; ζ-stat, n = 9.

active kinase and a postsynaptic scaffolding protein sustains late-LTP and long-term memory (Fig. 10). Our results reveal that coupling of PKMζ and KIBRA is necessary for long-term memory maintenance, providing a mechanism that also addresses the general question of how an increase in/activation of kinase signaling specifically targets action only at activated synapses. Thus, it is not PKMζ alone, nor KIBRA alone, but the interaction between the two that maintains LTP and memory (Figs. 4 to 9).

Synaptic stimulation that induces LTP facilitates the formation of KIBRA-PKMζ complexes that persist at least 3 hours in late-LTP maintenance (Fig. 1), and functional KIBRA-PKMζ coupling maintains late-LTP in hippocampal slices and memory lasting weeks in vivo (Figs. 4 to 9). This persistent coupling of KIBRA and PKMζ contrasts with the activities of other molecules that last for only seconds to minutes after strong synaptic stimulation, including CaMKII, cyclic adenosine monophosphate–dependent protein kinase, and most PKC isoforms (*11*, *43*, *44*), as well as local modulators of actin dynamics (*45*) and activators of gene expression that increase the synthesis of proteins cell-wide (*42*, *52*). These signaling molecules also act transiently for only minutes to hours during initial cellular memory consolidation (*44*, *45*, *52*), as compared to the persistent action of KIBRA-PKMζ coupling necessary for memory maintenance lasting weeks (Fig. 9B). Blocking PKMζ with antisense oligodeoxynucleotides or shRNA shows no effect on learning or initial short-term forms of memory while preventing long-term memory (*17*, *25*). Therefore, coupling PKMζ action to KIBRA is likely not essential for initial, transient forms of memory. KIBRA-PKMζ coupling, however, could play a role in the initiation of late-LTP and long-term memory, and this important question requires investigating the coupling during the formation of these fundamental processes.

We propose that KIBRA acts as a synaptic tag aligning PKMζ at activated synapses (Fig. 10). KIBRA interacts with postsynaptic α-amino-3-hydroxy-5-methyl-4-isoxazolepropionic acid receptors (AMPARs), functioning as a scaffolding protein to regulate trafficking of the receptors (*38*). Blocking PKMζ from binding the KIBRA tag during and after tetanization prevents the formation of late-LTP, allowing for early-LTP (Fig. 5B). Therefore, a simple hypothesis for the initiation of late-LTP is that the increased number of postsynaptic AMPARs in early-LTP sequesters KIBRA at activated synapses, and the scaffolding protein then acts as a tag at these synapses to anchor PKMζ (Fig. 10). Whether KIBRA accumulates at activated synapses first and PKMζ then binds the scaffolding protein or the proteins translocate to activated synapses as dimers (as shown in Fig. 10) requires further analysis of the translocation and complex formation of KIBRA and PKMζ in LTP induction. In LTP maintenance, both KIBRA and PKMζ are present in CA1 pyramidal cell somata, but they do not seem to be in a complex (Figs. 1B and 2A). This suggests that some other molecule, perhaps another PKC competing with PKMζ for KIBRA (fig. S3, A and B), is inhibiting their interaction in cell bodies. Alternatively, the soma might lack an element present at activated synapses that facilitates the alignment of KIBRA and PKMζ. One possible facilitating molecule is protein interacting with C kinase 1 (PICK1), which forms complexes with both KIBRA and PKMζ (*38*, *53*). PICK1, KIBRA, and PKMζ all regulate GluA2 subunit-dependent AMPAR trafficking (*38*, *53*–*55*). KIBRA also interacts with the actin-associated postsynaptic proteins, synaptopodin, angiomotin, and dendrin (*35*), as well as with other PKCs that are transiently activated in LTP (fig. S3, A and B) (*11*). In addition, KIBRA forms homodimers and also heterodimers with other members of the WWC family (*56*) and inducible genetic knockdown of KIBRA/WWC1 that suppresses LTP and memory formation down-regulates WWC2 as well, suggesting cooperative effects among WWC family members (*40*). Thus, KIBRA-PKMζ coupling might be a core interaction within a larger network of molecules that initiates "persistent synaptic tagging."

Once established, the continual alignment of KIBRA and PKMζ maintains late-LTP and long-term memory (Fig. 10). Antagonists that block the KIBRA-binding site in PKMζ or mimic the PKMζ-binding site in KIBRA reverse late-LTP at activated synapses when applied 3 hours after tetanization and have no measurable effect on unactivated, resting synaptic pathways in the same slice preparation (Figs. 4A and 8C) or on baseline synaptic transmission (Fig. 5B). These data support the specificity of the potentiating effects of

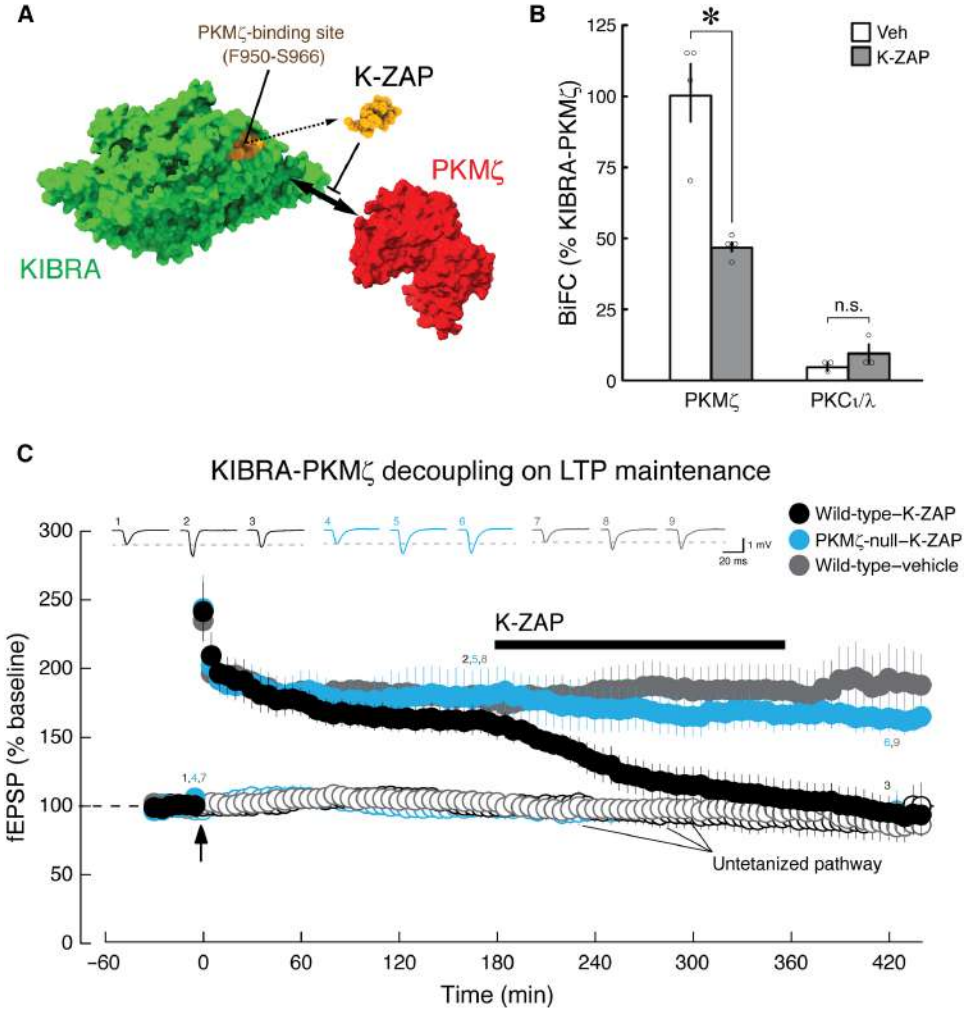

Fig. 8. K-ZAP peptide mimicking the PKMζ-binding site in KIBRA reverses late-LTP in wild-type mice but not in PKMζ-null mice. (**A**) Predicted structures show that K-ZAP mimics KIBRA PKMζ-anchoring site (orange). (**B**) BiFC reveals that K-ZAP (10 μM) inhibits PKMζ-KIBRA dimerization. KIBRA-PKCι/λ interactions are not measurably affected. Two-way ANOVA shows main effects of drug (K-ZAP/vehicle, $F_{1,10} = 14.59$, $P < 0.005$, $\eta^2_p = 0.59$), kinase ($F_{1,10} = 104.05$, $P < 0.00001$, $\eta^2_p = 0.91$), and interaction ($F_{1,10} = 19.98$, $P < 0.005$, $\eta^2_p = 0.67$). Post hoc analysis shows that K-ZAP suppresses KIBRA-PKMζ (*$P < 0.0005$), not KIBRA-PKCι/λ coupling ($P = 0.66$). K-ZAP/vehicle on KIBRA-PKMζ, *n*'s = 4; KIBRA-PKCι/λ, *n*'s = 3. (**C**) K-ZAP (10 μM) reverses late-LTP (black closed circles) with no effect on untetanized pathway (black open circles) or PKMζ-null (tetanized pathway, blue closed circles; untetanized pathway, blue open circles). Vehicle has no effect on wild-type–LTP (tetanized pathway, gray closed circles; untetanized, gray open circles). Tetanization at arrow. Top: numbered fEPSPs correspond to time points below. Repeated measures ANOVA shows group effect (wild-type with K-ZAP, PKMζ-null with K-ZAP, and wild-type with vehicle; $F_{2,9} = 4.43$, $P < 0.05$, $\eta^2_p = 0.50$), time effect (5 min before tetanization, 5 min before K-ZAP, and 1 hour after 3-hour K-ZAP application; $F_{2,18} = 43.46$, $P < 0.00001$, $\eta^2_p = 0.83$), and interaction ($F_{4,18} = 6.32$, $P < 0.005$, $\eta^2_p = 0.58$). Post hoc analysis reveals that K-ZAP disrupts established wild-type–LTP (5 min before tetanization versus 5 min before K-ZAP, $P < 0.005$; 5 min before K-ZAP versus 1 hour after 3-hour application of K-ZAP, $P < 0.005$). Wild-type–LTP remains intact in vehicle ($P < 0.0005$, $P = 0.77$, for equivalent time points). K-ZAP has no effect on PKMζ-null-LTP ($P < 0.0005$, $P = 0.21$, for equivalent time points). Wild-type/K-ZAP, $n = 4$; wild-type/vehicle, $n = 6$; PKMζ-null/K-ZAP, $n = 4$.

KIBRA-PKMζ coupling in activated synapses. The exclusive action of KIBRA-PKMζ inhibitors on late-LTP maintenance contrasts with CaMKII inhibitors, which either block LTP induction but not maintenance (*57*–*59*) or affect LTP within an hour of tetanization (*60*). In spatial memory, PKMζ increases selectively in subpopulations of neurons active during memory formation (marked by *Arc* promoter activation) and in subsets of synaptic spines of these active neurons (*19*). Further work is required to show coupling of the PKMζ to KIBRA specifically in activated synapses during memory storage by techniques such as enhanced green fluorescent protein reconstitution across synaptic partners (dual-eGRASP) (*61*).

Both antagonists of KIBRA-PKMζ coupling erase established late-LTP and long-term memory (Figs. 4A, 5A, 6, 7, 8C, and 9, and fig. S5); however, neither antagonist affects LTP or memory in PKMζ-null mice (Figs. 4B, 6, 7, 8C, and 9A). The PKMζ-independent maintenance of these mutant mice and also wild-type mice (fig. S6) could be through the prolonged actions of other PKCs (*17*), CaMKII (*60*), or other molecular mechanisms (*49*, *50*, *62*–*65*). The transient increase in PKCι/λ during early-LTP in wild-type mice becomes persistent during late-LTP in PKMζ-null mice (*17*). Whether KIBRA anchors and stabilizes PKCι/λ at activated synapses after genetic deletion of PKMζ remains to be explored but could provide a parsimonious account for

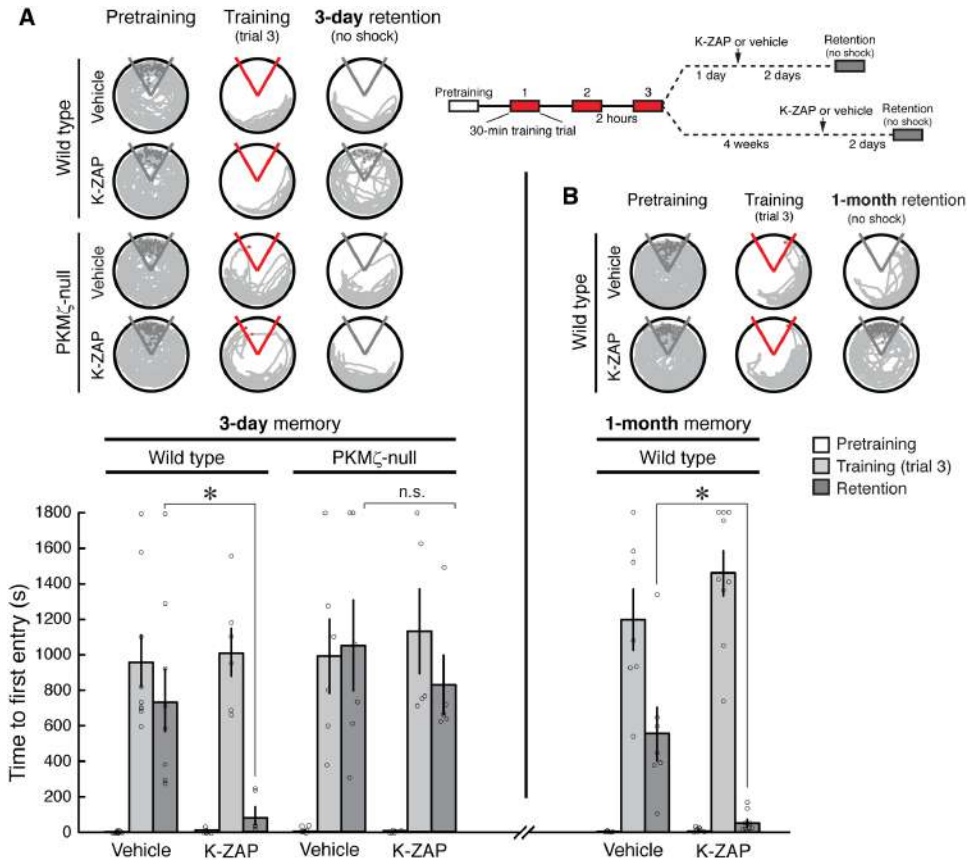

Fig. 9. K-ZAP peptide mimicking PKMζ-binding site in KIBRA disrupts long-term and remote spatial memory. Intrahippocampal injections of K-ZAP (5 nmol in 0.5 μl per side) disrupt maintenance of spatial memory measured (**A**) 3 days and, in separate experiments, (**B**) 30 days after conditioning. Top right (inset): schematic of active place avoidance protocol; injections are 2 days before memory retention testing for 3- and 30-day experiments. (A) Top: representative paths for 3-day memory conditioning during pretraining, the trial at end of training, and during retention testing with shock off 3 days after training. The shock zone is shown in red with shock on and gray with shock off. Red circles denote where shocks occur; gray circles denote where shocks would have been received if the shock were on. Bottom: means ± SEM. For 3-day memory, two-way ANOVA (drug and genotype) with repeated measurement (training phase) shows main effect of training phase ($F_{2,44} = 50.73$, $P < 0.00001$, $\eta^2_p = 0.70$) and interaction between training phase and drug ($F_{2,44} = 4.57$, $P < 0.02$, $\eta^2_p = 0.17$). Post hoc analysis reveals that wild-type mice receiving K-ZAP show loss of memory retention, compared to mice receiving vehicle (*$P < 0.01$), whereas PKMζ-null mice show intact memory retention whether receiving K-ZAP or vehicle ($P = 0.65$); wild-type mice: vehicle, $n = 8$; K-ZAP, $n = 6$; PKMζ-null mice: n's = 6. (B) Top: representative paths for 30-day memory. Bottom: one-way ANOVA with repeated measurement shows main effect of training phase ($F_{2,28} = 108.9$, $P < 0.00001$, $\eta^2_p = 0.89$) and interaction between training phase and drug ($F_{2,28} = 8.63$, $P < 0.001$, $\eta^2_p = 0.38$). Post hoc analysis reveals that mice receiving K-ZAP show loss of memory retention 30 days after training, compared to mice receiving vehicle (*$P < 0.005$); vehicle, $n = 7$; K-ZAP, $n = 9$.

compensation in PKMζ-null mutant mice. An initial, weak PKCι/λ interaction with KIBRA (Fig. 3B), which is displaced by the strong interaction of newly synthesized PKMζ in wild-type mice, might persist in the absence of PKMζ. A PKCι/λ inhibitor disrupts late-LTP and long-term memory maintenance exclusively in PKMζ-null mice and not wild-type mice (*17*). These pharmacogenetic experiments with ζ and ι/λ antagonists support (i) the KIBRA-PKMζ maintenance hypothesis that late-LTP and long-term memory in wild-type mice share a common PKMζ-dependent molecular mechanism of information storage (*7*) and (ii) mutant mice lacking PKMζ recruit compensatory PKMζ-independent maintenance mechanisms (*17*).

The persistent anchoring of PKMζ by KIBRA at activated synapses that maintains physiological long-term memory could help explain how overexpression of PKMζ and KIBRA can enhance memory. PKMζ overexpression after memory formation enhances weak long-term memories that have faded over time (*31*). This result was unexpected because overexpressed PKMζ might enhance synapses indiscriminately and, as a consequence, degrade information stored by differences in synaptic weights in neuronal circuits (*3*, *29*, *30*). Our findings, however, suggest the possibility that the overexpressed PKMζ might target KIBRA at appropriate activated synapses to replace the endogenous PKMζ that, like synaptic potentiation (*26*), declines as memories fade (*18*). Likewise, in a mouse model of the human tauopathy associated with Alzheimer's disease, the endogenous KIBRA is deficient in anchoring PKMζ, and overexpression of a fragment of KIBRA that traffics to synapses and binds PKMζ restores the ability to form long-term memory (*66*). Our results suggest that providing the fragment of KIBRA reconstitutes the physiological link between activated synapses and PKMζ's potentiating action, thus overcoming the defective PKMζ anchoring in the tauopathy of Alzheimer's disease.

The persistent coupling of KIBRA to PKMζ's potentiating action at activated synapses maintains memory longer than the predicted life spans of individual KIBRA (*28*, *39*, *40*) and PKMζ molecules (*24*, *25*) (Fig. 9B and fig. S8). Thus, as in Crick's hypothesis, the molecules

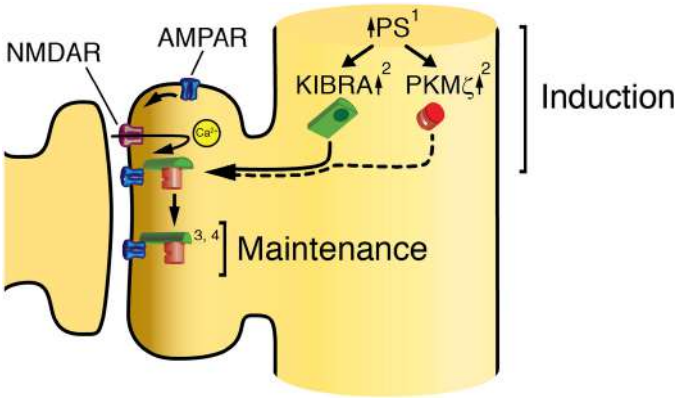

Fig. 10. Schematic illustration of signaling pathways for KIBRA-PKMζ interaction in the induction and maintenance of late-LTP and long-term memory. In induction, high-frequency afferent synaptic stimulation activates postsynaptic *N*-methyl-D-aspartate receptors (NMDARs), and the resulting influx of postsynaptic Ca^{2+} initiates early-LTP and (1) increases protein synthesis (PS), which may be localized in dendrites. The enhanced synthesis results in (2) increased amounts of the postsynaptic scaffolding protein KIBRA, which interacts with AMPARs, and the persistently active kinase PKMζ (Fig. 2). We hypothesize that, in early-LTP, trafficking of extrasynaptic AMPARs to postsynaptic sites sequesters KIBRA at activated synapses. In late-LTP induction, KIBRA can then act as a synaptic tag to bind PKMζ, shown here interacting with AMPARs as a KIBRA-PKMζ dimer. In late-LTP maintenance, (3) postsynaptic KIBRA and PKMζ form persistent KIBRA-PKMζ complexes (Fig. 1). (4) Decoupling KIBRA from PKMζ reverses late-LTP maintenance at activated synapses (Figs. 4A, 5A, and 8C) and disrupts long-term memory maintenance for at least 4 weeks (Fig. 9B). This duration of memory is longer than the life spans of individual KIBRA (*28*, *39*, *40*) and PKMζ molecules (*24*, *25*) (fig. S8). Therefore, the components of the complex are likely replaced by newly synthesized molecules.

of KIBRA and PKMζ must be replaced with new molecules, and these newly synthesized proteins must be targeted to appropriate sites at activated synapses. The degrading KIBRA and PKMζ are likely exchanged by new molecules produced by local dendritic synthesis from PKMζ mRNA (*15*) and perhaps KIBRA mRNA as well (*67*). A positive feedback loop by which PKMζ up-regulates dendritic synthesis, including that from its own mRNA, has been reported (*68*, *69*). KIBRA anchoring PKMζ's action may further localize this dendritic synthesis to activated synapses.

The KIBRA-PKMζ complexes in activated synapses might then align the newly synthesized KIBRA and PKMζ with the synapses' AMPAR trafficking machinery in a self-perpetuating molecular mechanism. The autonomous activity of PKMζ sustains synaptic potentiation by increasing the number of postsynaptic AMPARs (*5*, *6*). This action is through persistently decreasing the endocytosis of recycling GluA2 subunit-containing AMPARs (*53*, *55*). These AMPAR subunits interact with KIBRA (*38*). Therefore, we speculate that, in a process distinct from the initial setting of the tag that establishes the commitment to late-LTP (*42*, *70*), the continual accumulation of KIBRA at potentiated synapses serves as a persistent synaptic tag in late-LTP maintenance for newly synthesized PKMζ (*8*). The antagonists that block formation of KIBRA-PKMζ complexes (Figs. 3 and 8, A and B) reverse established late-LTP within a few hours of their application (Figs. 4A, 5A, and 8C). Therefore, the exchange of complexes within activated synapses may be rapid. However, we do not know if the antagonists might also disrupt established complexes. This is because the reconstitution of split-Venus used in the BiFC assay to test the inhibitors is likely irreversible (*71*). The question of the rate of complex turnover in activated synapses can be investigated by the development of technologies such as live-imaging dual-eGRASP that could identify these synapses in vivo (*61*). Nonetheless, both KIBRA (*28*, *39*, *40*) and PKMζ (*24*, *25*) (fig. S8) appear from knockdown experiments to turn over in neurons within hours to days, while KIBRA-PKMζ interactions sustain memory for at least 4 weeks (Fig. 9B). Thus, as Theseus' Ship was sustained for generations by continually replacing worn planks with new timbers (*72*), long-term memory can be maintained by continual exchange of potentiating molecules at activated synapses, a concept we call persistent synaptic tagging.

MATERIALS AND METHODS

Experimental design

Reagents

Unless otherwise stated, reagents were from MilliporeSigma. ζ-stat (NSC 37044) was obtained from Drug Synthesis and Chemistry Branch, Developmental Therapeutics Program, Division of Cancer Treatment and Diagnosis, National Cancer Institute. Upon arrival, the drug was dissolved in phosphate-buffered saline (PBS) (pH 7.4), aliquoted at 10 mM stock solution, and stored at −20°C. K-ZAP (myr-N-FVRNSLERRSVRMKRPS-C) was custom-synthesized by AnaSpec (Fremont, CA) and stored in PBS (pH 7.4) at −20°C.

Animals and cell lines

This study was performed in strict accordance with the recommendations in the Guide for the Care and Use of Laboratory Animals of the National Institutes of Health. All animals were handled according to approved Institutional Animal Care and Use Committee (IACUC) protocols [no. 11-10274, 15-10467 of the State University of New York (SUNY) Downstate Health Sciences University, or 2000-4512 of McGill University]. The protocols were approved by the IACUC of SUNY Downstate Health Sciences University (animal welfare assurance number: D16-00167) and McGill University (animal welfare assurance number: F16-00005). All efforts were made to minimize animal suffering and to reduce the number of animals used. C57/B6 mice and PKMζ-null mice on a C57/B6 background at SUNY Downstate Health Sciences University were genotyped as previously described (*17*). PKMζ-null mice at McGill University were a generous gift from W. Sossin, Montreal Neurological Institute, McGill University. *Prkcz*$^{fl/fl}$ mice were a generous gift from S. Ghosh, Yale University. Male mice were examined in this study, and KIBRA-PKMζ interaction in LTP and memory maintenance in both sexes will be compared in a future study. HEK293T cell line was obtained from the ATCC (American Type Culture Collection).

Hippocampal slice recording and stimulation

Acute mouse hippocampal slices (450 μm) were prepared as previously described (*17*, *73*). Hippocampi from 2- to 6-month-old male C57/B6 or PKMζ-null mice as previously described (*17*) were dissected, bathed in ice-cold dissection buffer, and sliced with a McIlwain tissue slicer in a cold room (4°C). The dissection buffer contained 125 mM NaCl, 2.5 mM KCl, 1.25 mM NaH_2PO_4, 26 mM $NaHCO_3$, 11 mM glucose, 10 mM $MgCl_2$, and 0.5 mM $CaCl_2$ and was bubbled with 95% O_2/5% CO_2 to maintain pH at 7.4. After dissection, the slices were immediately transferred into an Oslo-type interface recording chamber (31.5° ± 1°C) (*73*). The recording superfusate consisted of 118 mM NaCl, 3.5 mM KCl, 2.5 mM $CaCl_2$, 1.3 mM $MgSO_4$, 1.25 mM NaH_2PO_4, 24 mM $NaHCO_3$,

and 15 mM glucose, bubbled with 95% O_2/5% CO_2, with a flow rate of 0.5 ml/min. In a subset of experiments, a custom-made recirculation system using piezoelectric pumps was used for recycling the superfusate (Bartels Mikrotechnik GmbH, Dortmund, Germany) (*73*).

fEPSPs were recorded with a glass extracellular recording electrode (2 to 5 megohms) placed in the CA1 st. radiatum, and concentric bipolar stimulating electrodes (CBBRE75 and 30200; FHC, Bowdoin, ME) were placed on either side within CA3 or CA1. Test stimulation rate was once every 30 s, alternating every 15 s between stimulating electrodes. Based on a preestablished exclusion criterion, a slice was not used if fEPSP spike threshold was <2 mV on initial input-output analysis. Pathway independence was confirmed by the absence of paired-pulse facilitation between the two pathways. A single stimulating electrode was used for PLA/immunocytochemistry with a test stimulation rate of once every 30 s. The high-frequency stimulation, optimized to produce a relatively rapid onset of protein synthesis-dependent late-LTP (*74*), consisted of two 100-Hz/1-s tetanic trains, at 25% of spike threshold, spaced 20 s apart. The maximum slope of the rise of the fEPSP was analyzed on a PC using the WinLTP data acquisition program (*75*).

Proximity ligation assay

Methods used were as described in the Sigma Duolink PLA Probemaker Guide (MilliporeSigma, St. Louis, MO). Because PLA is highly sensitive, standard immunocytochemical blocking methods used to detect independent fluorescent signals from two primary antisera of the same species (fig. S1B) may not be sufficient; therefore, anti-PKMζ–PLUS and anti-KIBRA–MINUS probes were generated by directly conjugating the individual rabbit primary antibodies [C2 (*12*, *19*) and ab216508, Abcam, Waltham, MA] with PLA oligonucleotides (PLUS and MINUS, respectively). Briefly, following purification with Microcon Centrifugal Filters (Millipore, Burlington, MA), the carrier- and preservative-free anti-PKMζ and anti-KIBRA primary antibodies (1 mg/ml in PBS) were incubated with lyophilized nucleotides (PLUS or MINUS, respectively) at 20°C overnight. The reaction was terminated by incubation with the Stop Reagent for 30 min at 20°C, and an equal total volume of Storage Solution was added.

Hippocampal slices were fixed by immersion in ice-cold 4% paraformaldehyde in 0.1 M phosphate buffer (PB) (pH 7.4) immediately after recording and postfixed for 48 hours. Slices were then washed with PBS (pH 7.4) and cut into 20 μM sections using a Leica VT 1200S vibratome. Free-floating sections were permeabilized in 96-well plates with PBS-TX100 for 6X 10 min at 20°C and blocked with Duolink Blocking Solution (Sigma-Aldrich, DUO82007-8 ml) for 1 hour at 37°C in a preheated humidity chamber. The sections were then incubated overnight at 4°C with anti-PKMζ–PLUS probe (1:400) and anti-KIBRA–MINUS probe (1:400) mixed in Duolink Probe Diluent. After 6X 10-min washes with Duolink In Situ Buffer A, the sections were incubated in a preheated humidity chamber for 30 min at 37°C with Ligation Buffer (5X Duolink Ligation buffer diluted 1:5 in high-purity water) containing the Ligase enzyme. Following 6X 10-min washes with Duolink In Situ Buffer A, the sections were incubated in a preheated humidity chamber for 100 min at 37°C with Amplification Buffer (5X Duolink Amplification buffer diluted 1:5 in high-purity water) containing Polymerase enzyme (Duolink In Situ Detection Reagents Red; Sigma-Aldrich, DUO92008). The sections were then washed for 6X 10 min with Duolink In Situ Buffer B at 20°C, followed by a 1-min wash in 0.01X Wash Buffer B. The sections were mounted with Sigma-Aldrich Duolink In Situ Mounting Medium containing 4′,6-diamidino-2-phenylindole (DAPI) (DUO82040). A single confocal plane consisting of individual tiles was captured using the Tiles tool of a Zeiss LSM800 AxioObserver Z1/7 confocal microscope with a Plan-Apochromatic 20X/0.8 M27 lens. For each fluorophore, all parameters (pinhole, excitation wavelength, emission power, and detector gain) were held constant for all imaging sessions. To correct for tiling artifacts that result from uneven illumination, an estimated shading profile was calculated for each channel with the BaSiC tool for illumination correction, using an ImageJ/Fiji Plugin (https://github.com/marrlab/BaSiC) (*76*). Shading correction was applied in Zen 2.6 software using the "Shading Correction" function. In a subset of experiments when conjugating MINUS probe was unavailable from the manufacturer, the anti-KIBRA–MINUS probe was substituted with a biotinylated (Abcam Lightning-Link ab201795) anti-KIBRA ab216508 primary (1:400 in Duolink Antibody Diluent; incubated overnight at 4°C). After 6X 10-min washing (Duolink In Situ Buffer A), a goat anti-biotin secondary (1:200 in Antibody Diluent; Sigma-Aldrich, B3640-1MG) was applied for 2 hours at 20°C. After another 6X 10-min washing, the sections were incubated with Duolink PLA donkey anti-goat (DAG)–minus (1:5; DUO92003) in Antibody Diluent at 37°C for 1 hour. Both methods yielded similar results.

Immunocytochemistry

Hippocampal slices were fixed by immersion in ice-cold 4% paraformaldehyde in 0.1 M PB (pH 7.4) immediately after recording and postfixed for 48 hours. Slices were then washed with PBS (pH 7.4) and cut into 20 μM sections using a Leica VT 1200S vibratome. Free-floating sections were permeabilized in 96-well plates with PBS containing 0.3% Triton X-100 (PBS-TX100) for 6X 10 min at 20°C and blocked with 10% normal donkey serum in PBS-TX100 for 2.5 hours at 20°C. The sections were then incubated overnight at 4°C with primary rabbit anti-KIBRA antibody (ab216508, Abcam, Waltham, MA) at 1:100 in PBS-TX100. After washing 6X 10-min in PBS-TX100 at 20°C, the sections were incubated with Alexa Fluor 488–conjugated donkey anti-rabbit (1:200 in PBS-TX100; Jackson ImmunoResearch, West Grove, PA) for 2 hours at 20°C. After 6X 10-min washes in PBS-TX100 at 20°C, the slices were blocked for 2 hours at 20°C with 5% normal rabbit serum in PBS-TX100, followed by 6X 10-min washes in PBS-TX100 at 20°C. The slices were then further blocked with 10% AffiniPure Fab Fragment donkey anti-rabbit IgG H+L (Jackson ImmunoResearch) PBS-TX100 for 2 hours at 20°C. This additional blocking step was followed by 6X 10-min washes in PBS-TX100 at 20°C. The sections were then incubated overnight at 4°C with primary antibody rabbit anti-PKCζ/PKMζ C2 [1:4000 (*19*); generated as previously described (*12*)] in PBS-TX100. After 6X 10-min washes in PBS-TX100 at 20°C, the sections were incubated with Alexa Fluor 647–conjugated donkey anti-rabbit (1:200 in PBS-TX100; Jackson ImmunoResearch) for 2 hours at 20°C. After washing 6X 10-min in PBS-TX100, the sections were incubated with streptavidin-conjugated Alexa Fluor 647 (1:250 in PBS-TX100; Jackson ImmunoResearch) for 2 hours at 20°C. After 6X 10-min washes at 20°C with PBS-TX100 and 10 min with PBS, the sections were mounted with DAPI Fluoromount-G (Southern Biotech). This procedure produces no bleedthrough between KIBRA and PKMζ fluorescent signals (fig. S1B). A single confocal plane consisting of individual tiles was captured using the Tiles tool of a Zeiss LSM800 AxioObserver Z1/7 confocal microscope with a Plan-Apochromatic 20X/0.8 M27 lens. For each fluorophore, all parameters (pinhole, excitation wavelength, emission power, and detector gain) were held constant for all imaging sessions. To correct

for tiling artifacts that result from uneven illumination, an estimated shading profile was calculated for each channel with the BaSiC tool for illumination correction, using an ImageJ/Fiji Plugin (https://github.com/marrlab/BaSiC) (*76*). Shading correction was applied in Zen 2.6 software using the Shading Correction function.

Three-dimensional protein modeling

Molecular graphics performed with UCSF ChimeraX (version 1.6.1), developed by the Resource for Biocomputing, Visualization, and Informatics at the University of California, San Francisco, with support from National Institutes of Health R01.GM129325 and the Office of Cyber Infrastructure and Computational Biology, National Institute of Allergy and Infectious Diseases (*77*, *78*). The simulated protein models of KIBRA and PKMζ for illustration are developed by ModBase (*79*) and T. Ko at the University of Pennsylvania, respectively.

BiFC assay

Transfection constructs. KIBRA-PKMζ BiFC was performed as previously described (*28*), using pVen1-FLAG-KIBRA and pVen2-HA-PKMζ, in which PKMζ was cloned between Eco RI and Bam HI sites. The constructs pVen1 and pVen2 encode the N terminus (amino acids 1 to 154) and C terminus (amino acids 155 to 238) of the Venus protein, respectively, and the Venus fragments were on the N terminus of the fusion proteins. pVen2-HA-PKMζ[PKCι/λ-P291Q;F297S] was generated by site-directed mutagenesis using forward (cctggagAagcAAatccggatcccccggtCcctgtccgtc) and reverse (gacggacaggGaccgggggatccggatTTgctTctccagg) primers and the QuickChange II XL Site-Directed Mutagenesis Kit (Agilent Technologies), following manufacturer's instructions. Additional pVen2-HA-PKC isoforms and pVen2-HA-CaMKIIα in the pVen2-HA vector were generated by cloning the N terminus of the coding sequence of each kinase (table S1) to obtain an in-frame fusion at the C terminus of the pVen2-HA. Human versions of KIBRA and kinases were used, and all polymerase chain reaction amplified sequences and constructs were verified by DNA sequencing.

Cell culture and transfection. HEK293T cells were cultured in Dulbecco's modified Eagle's medium supplemented with 10% heat-inactivated fetal bovine serum, penicillin (100 U/ml), streptomycin (100 mg/ml), 2 mM glutamine, and 10 mM Hepes in a T75 tissue culture flask with canted neck and ventilated cap. Twenty-four hours prior to transfection, 1×10^5 HEK293T cells in 1 ml of media were plated on poly-D-lysine–treated coverslips in 24-well plates. One hour prior to transfection, 0.5 ml of the media was removed from each well, and ζ-stat or K-ZAP was added to the media that had been removed. The remaining media in each well was then discardeXd and substituted with the 0.5-ml preconditioned media containing ζ-stat or K-ZAP at designated concentrations. For transfection, a total of 50 ng of DNA was delivered to each well using Lipofectamine 3000 (Invitrogen) and OptiMEM 1X reduced serum medium (Invitrogen) at a plasmid-to-plasmid ratio of 1:1. The amount of transfected DNA was optimized to produce relatively low concentrations of proteins during overexpression. The cells were cotransfected with pVen1-FLAG-KIBRA and pVen2-HA-PKMζ, as previously described (*28*), or pVen1-FLAG-KIBRA and pVen2-HA-PKMζ[PKCι/λ-P291Q;F297S]/PKC isoforms/CaMKIIα. As controls, cells were cotransfected with pVen1-FLAG-KIBRA and pVen2-HA or pVen1-FLAG and pVen2-HA-PKMζ. After transfection, the cells were incubated for 24 hours, fixed with 4% paraformaldehyde, and kept on 0.02% sodium azide in 1X PBS at 4°C until immunostaining.

Immunostaining and confocal microscopy. To detect FLAG and HA tags in cells transfected with BiFC plasmids, the cells were blocked and permeabilized using blocking buffer (2% bovine serum albumin, 0.05% Tween 20, and 0.1% Triton X-100 in 1X PBS) for 15 min at 20°C. The primary antibodies, mouse anti-FLAG (1:100, Sigma-Aldrich) and rabbit anti-HA (1:100, Sigma-Aldrich), were diluted in blocking buffer. The blocking solution was then removed, 200 μl of the diluted primary antibody was added to each well, and the samples were incubated overnight at 4°C. The primary antibody was then removed, followed by 3X 5-min washes with 0.05% Tween 20 in 1X PBS. The cells were then incubated for 1 hour in the dark at 20°C with secondary antibodies, Alexa Fluor 647–conjugated goat anti-mouse (1:250, Invitrogen) and Alexa Fluor 594–conjugated goat anti-rabbit (1:250, Invitrogen) diluted in blocking buffer. The secondary antibody solution was removed, and the same washing steps as with the primary antibody solution were performed. The cells were mounted on glass slides with DAPI Fluoromount-G (Southern Biotech). Z-stack images of random microscopic fields were acquired with a 1-μm z-step on a confocal microscope Zeiss LSM800 AxioObserver Z1/7 using a Plan-Apochromatic 63X/1.4 NA (numerical aperture) oil objective and exported as maximum intensity projection. All imaging parameters (pinhole, excitation wavelength, emission power, and detector gain) were constant for all experimental conditions. To determine the number of interacting BiFC puncta per cell, the images were converted to grayscale and the ImageJ 1.52n (*80*) freehand or wand selection tools were used to create an outline of each cell, which was added to the region of interest manager. To ensure that HEK293T cells were transfected with both pVen1-FLAG-KIBRA and pVen2-HA-PKMζ (or pVen1-FLAG-KIBRA and pVen2-HA-PKMζ[PKCι/λ-P291Q;F297S]/PKC isoforms/CaMKIIα), only cells that were positive for FLAG and HA tags signals were included in the analysis. The "find maxima" algorithm from ImageJ was used to count the number of local maxima per cell with a noise tolerance of 10, as previously described (*81*). Individual data points for each experimental condition (control and treatment) consist of the means of >50 cells obtained from two independent cultures.

Behavior—Active place avoidance

Intrahippocampal injection. For spatial long-term memory experiments, we adapted the approach used by Garcia-Osta *et al.* (*82*). Mice were ~12 weeks old at surgery. Briefly, to implant the injection cannula hardware, mice were anesthetized by an intraperitoneal injection of a mixture of dexmedetomidine (5 mg/kg body weight) and ketamine (28 mg/kg body weight) and mounted in a Kopf stereotaxic frame (Tujunga, CA). The tips of guide cannula (Plastics One, Roanoke, VA; part number: C235GS-5-2.0) were targeted above the injection target in the dorsal hippocampus [anterior/posterior (AP), −1.94 mm; medial/lateral(ML), ±1.00 mm; dorsal/ventral (DV), −0.90 mm]. The other injection hardware (part numbers: C235DCs-5 and 303 DC/1; cannula dummy and cannula cap, respectively) was assembled, and antisedan (0.65 mg/kg body weight, intraperitoneally) was administered to reverse the sedation at the end of surgery.

Three to 4 weeks after surgery, the animals received active place avoidance training. Before testing the effect of the drug injection on place avoidance, the animals received a bilateral injection of vehicle [PBS (pH 7.4), 0.5 μl per side] and were left in the home cage to habituate to the procedure. Depending on the experimental

design, injection of vehicle or drug, either ζ-stat or K-ZAP (5 nmol in 0.5 μl of PBS per side), is 1 day or 4 weeks after the training session. During the injection, the animals were restrained, the cannula cap and dummy were removed, and the injection needle (Plastics One, Roanoke, VA; part number: C235IS-5) was inserted into the guide cannula so that it protruded from the end of the guide by 0.5 mm. The other end of the needle was connected to a 10-μl Hamilton syringe via Tygon tubing. The drug or vehicle was infused for 1 min, and after the infusion, the needle was left in place for 5 min before removal. The animals were then returned to their home cages until the memory retention tests that were conducted 2 days later.

Conditioning. Active place avoidance was conducted with a commercial computer-controlled system (Bio-Signal Group, Acton, MA). The mouse was placed on a 40-cm diameter circular arena rotating at 1 rpm. The specialized software, Tracker (Bio-Signal Group, Acton, MA), was used to detect the animal's position 30 times per second by video tracking from an overhead camera. A clear wall made from PET-G (polyethylene terephthalate glycol–modified) was placed on the arena to prevent the animal from jumping off the elevated arena surface. A 5-pole shock grid was placed on the rotating arena, and the shock was scrambled across the 5 poles when the mouse entered the shock zone. All experiments used the "Room+Arena-" task variant that challenges the mouse on the rotating arena to avoid a shock zone that was a stationary 60° sector (*7*). Every 33 ms, the software determined the mouse's position, whether it was in the shock zone and whether to deliver shock. After the animal enters the shock zone for 500 ms, a constant current footshock (60 Hz, 500 ms) was delivered and repeated with the interval of 1500 ms until the mouse left the shock zone. The shock intensity was 0.2 or 0.3 mA, which was the minimum amplitude to elicit flinch or escape responses. The animal was forced to actively avoid the designated shock zone because the arena rotation periodically transported it into the shock area.

The tracked animal positions with timestamps were analyzed offline (TrackAnalysis, Bio-Signal Group, Acton, MA) to extract several end-point measures. The time to first enter the shock zone estimates ability to avoid shock and was taken as an index of between-session memory. The number of entrances within one trial was taken as another index to examine the animal learning curve throughout all training trials. A pretraining habituation period on the apparatus equivalent in time to a training session, but without shock, was provided.

The training schedule was as follows: 2 hours after a 30-min pretraining habituation, the animals received three 30-min training trials, with an intertrial interval of 2 hours. Bilateral intrahippocampal injection of ζ-stat or vehicle (Fig. 6) or K-ZAP or vehicle (Fig. 9) was 24 hours (Figs. 6 and 9A) or 4 weeks (Fig. 9B) after the training session. Retention testing was a 30-min trial without shock 2 days after injection. In fig. S5, the animals first received the conditioning in context A, injection, and a memory retention test as described above. Immediately after retention testing, the animals were conditioned in context B with a different set of spatial cues, and memory for active place avoidance in context B was tested 3 days later. Preestablished exclusion criterion was if, after sacrificing the animals and performing histology for cannula placement, cannulae were found to be incorrectly targeted. The data from two animals were excluded from behavioral analysis of the effects of ζ-stat on PKMζ-null mice because histology revealed misplaced cannulae.

Behavior—Auditory-cued fear/threat conditioning

Animals. Mice were 8 to 10 weeks old at the time of cannulation and 9 to 11 weeks old at the beginning of behavioral experiments. Mice were housed with cage mates in plastic cages and provided with food and water ad libitum. Mice were maintained on a 12-hour:12-hour light:dark cycle (lights on at 7:00 a.m.) and behavioral experiments began at 9:00 a.m.

Surgery. Mice were injected intraperitoneally (1 ml/100 g body weight) with an anesthetic cocktail containing ketamine (10 mg/ml) and xylazine (2 mg/ml). Mice were provided with analgesic treatment prior to surgery (carprofen; 5 mg/ml). Guide cannulae (Plastics One, Roanoke, VA) were implanted bilaterally in the BLA (from bregma: AP, −1.7 mm; ML, ±3.0 mm; DV, −4.4 mm) and secured to the skull with three jeweler's screws and dental cement. Antisedan (0.66 ml/100 g body weight of 0.5 mg drug per ml solution) was given via intraperitoneal injection after surgery to reverse the anesthesia.

Conditioning. For 7 days following surgery, mice were handled by freely exploring the experimenter's palm for 2 to 5 min. Mice were habituated, trained, and tested in the same conditioning box (Coulbourn Habitest, Coulbourn Instruments) with differing floors and walls to produce two different contexts (context A and context B). For each day of the behavioral experiment, mice were brought to the experiment room at 9:00 a.m. and allowed to acclimatize for 30 min. Mice were then habituated to the testing context (context A with smooth floor and flat, blank walls) for 20 min each day for two consecutive days. The next day, mice were trained in a second context (context B with a grid floor, patterned walls, and a curved wall). Training consisted of 2 min of exploration of context B followed by a tone (2800 Hz, 85 dB, and 30 s) coterminating with a footshock (0.7 mA, 1 s). Mice received two tone-shock pairings separated by 1 min and remained in context B for an additional 1 min before returning to their home cage. Mice were tested 24 hours after training in context A (test 1). During testing, mice were placed in the conditioning box and, after 2 min, were exposed to a 30-s tone (2800 Hz, 85 dB). The next day, mice received bilateral infusions and were tested a second time 24 hours after infusion in context A (test 2). Freezing behavior (cessation of all movement except breathing) during the tone on test 1 and test 2 was scored by an experimenter blind to the conditions. Scores are reported as the percent of time spent freezing during the tone. Preestablished exclusion criteria were (i) if the mouse froze less than 25% of the time after the conditioned stimulus was presented at the first test, which is the standard cutoff used in the Nader lab to distinguish mice that had learned or not learned the conditioned stimulus-unconditioned stimulus association; and (ii) if after sacrificing the animals and performing histology for cannula placement, cannulae were found to be incorrectly targeted.

Drug infusions. Mice were bilaterally infused with ζ-stat obtained from Drug Synthesis and Chemistry Branch, National Cancer Institute or vehicle [PBS (pH 7.4)]. Mice were infused with 6 nmol of ζ-stat in 0.3 μl at a rate of 0.2 μl/min into each BLA. Drugs were infused with 28-gauge microinjectors (Plastics One, Roanoke, VA) connected to Hamilton syringes (26 gauge, model 1701N) by way of polyethylene tubing (Braintree Scientific Inc., Braintree, MA). After infusion, injectors remained in place for 1 min to ensure that drug diffused sufficiently away from the injector tip.

Behavior—Contextual fear/threat conditioning

Animals. Mice were 8 to 10 weeks old at the time of cannulation and 9 to 11 weeks at the beginning of behavioral experiments. Mice were housed with cage mates in plastic cages and provided with food and water ad libitum. Mice were maintained on a 12 hours light/dark cycle (lights on at 7:00 a.m.) and behavioral experiments began at 9:00 a.m.

Surgery. Mice were injected intraperitoneally (1 ml/100 g body weight) with an anesthetic cocktail containing ketamine (10 mg/ml) and xylazine (2 mg/ml). Mice were provided with analgesic treatment prior to surgery (carprofen; 5 mg/ml). Guide cannulae (Plastics One, Roanoke, VA) were implanted bilaterally in the dorsal hippocampus (from bregma: AP, −2.1 mm; ML, ±1.8 mm; DV, −1.2 mm) and secured to the skull with three jeweler's screws and dental cement. Antisedan (0.66 ml/100 g body weight of 0.5 mg drug per ml solution) was given via intraperitoneal injection after surgery to reverse the anesthesia.

Conditioning. For 7 days following surgery, mice were handled by freely exploring the experimenter's palm for 2 to 5 min. Mice were trained and tested in the same conditioning box (Coulbourn Habitest, Coulbourn Instruments), which consisted of a grid floor and blank walls. For each day of the behavioral experiment, mice were brought to the experiment room at 9:00 a.m. and allowed to acclimatize for 30 min. On the first day (training), mice explored the context for 2 min. We then delivered two 0.7-mA (1-s) shocks spaced 1 min apart. Mice remained in the box for an additional minute before returning to their home cage. The next day, mice received bilateral infusions and were tested 24 hours after infusion. During testing, mice were placed in the same context for 4 min with no shock. Freezing behavior (cessation of all movement except breathing) during the 4-min session was recorded by an experimenter blind to the conditions. Scores are reported as the percent of time spent freezing during the 4-min session. Preestablished exclusion criterion was if, after sacrificing the animals and performing histology for cannula placement, cannulae were found to be incorrectly targeted.

Drug infusions. Mice were bilaterally infused with vehicle [PBS (pH 7.4)] or ζ-stat (10 nmol in 0.5 μl per hemisphere at a rate of 0.2 μl/min per side). Drugs were infused with 28-gauge microinjectors (Plastics One, Roanoke, VA) that protruded 0.3 mm from the guide cannulae connected to Hamilton syringes (26 gauge, model 1701N) by way of polyethylene tubing (Braintree Scientific Inc., Braintree, MA). After infusion, injectors remained in place for 1 min to ensure drug diffusion away from the injector tip.

Immunoblotting

Immunoblots for fig. S8 were performed as previously described (*19*).

Statistical analysis

Replicates are biological because there is only one measurement for each sample. Drug/vehicle comparisons were performed blindly. Sample sizes vary for the different experimental approaches (biochemistry, slice physiology, and behavior) and were established by power analyses based on effect size estimates from published works or preliminary experiments. The observed effect sizes for binary comparisons are reported as Cohen's d and as η^2_p for ANOVA effects. Multifactor comparisons were performed using ANOVA with repeated measures, as appropriate. Two-population Student's t tests were performed to compare protein immunofluorescence intensity between control and potentiated hippocampal slices. For LTP experiments, the responses were first normalized to the mean of the 30-min period prior to tetanization (or equivalent in control pathways), and then the means over 5-min periods were used for statistical comparisons (e.g., pretetanization and beginning and end of drug application). Paired Student's t tests were used to compare the change in the potentiated response at time points at the beginning and end of drug application. The degrees of freedom for the critical t values of the t tests and the F values of the ANOVAs are reported as subscripts. Post hoc multiple comparisons were performed by Newman-Keuls tests as appropriate. Statistical significance was accepted at $P < 0.05$ or appropriate Bonferroni correction for multiple comparisons.

Supplementary Materials

This PDF file includes:

Figs. S1 to S8
Table S1

REFERENCES AND NOTES

1. F. Crick, Neurobiology: Memory and molecular turnover. *Nature* **312**, 101 (1984).
2. J. E. Lisman, A mechanism for memory storage insensitive to molecular turnover: A bistable autophosphorylating kinase. *Proc. Natl. Acad. Sci. U.S.A.* **82**, 3055–3057 (1985).
3. S. J. Martin, P. D. Grimwood, R. G. Morris, Synaptic plasticity and memory: An evaluation of the hypothesis. *Annu. Rev. Neurosci.* **23**, 649–711 (2000).
4. T. V. P. Bliss, T. Lømo, Long-lasting potentiation of synaptic transmission in the dentate area of the anaesthetized rabbit following stimulation of the perforant path. *J. Physiol.* **232**, 331–356 (1973).
5. D. S. Ling, L. S. Benardo, P. A. Serrano, N. Blace, M. T. Kelly, J. F. Crary, T. C. Sacktor, Protein kinase Mζ is necessary and sufficient for LTP maintenance. *Nat. Neurosci.* **5**, 295–296 (2002).
6. D. S. Ling, L. S. Benardo, T. C. Sacktor, Protein kinase Mζ enhances excitatory synaptic transmission by increasing the number of active postsynaptic AMPA receptors. *Hippocampus* **16**, 443–452 (2006).
7. E. Pastalkova, P. Serrano, D. Pinkhasova, E. Wallace, A. A. Fenton, T. C. Sacktor, Storage of spatial information by the maintenance mechanism of LTP. *Science* **313**, 1141–1144 (2006).
8. T. C. Sacktor, How does PKMζ maintain long-term memory? *Nat. Rev. Neurosci.* **12**, 9–15 (2011).
9. P. W. Frankland, S. A. Josselyn, Neuroscience: Memory and the single molecule. *Nature* **493**, 312–313 (2013).
10. T. C. Sacktor, A. A. Fenton, What does LTP tell us about the roles of CaMKII and PKMζ in memory? *Mol. Brain* **11**, 77 (2018).
11. T. C. Sacktor, P. Osten, H. Valsamis, X. Jiang, M. U. Naik, E. Sublette, Persistent activation of the zeta isoform of protein kinase C in the maintenance of long-term potentiation. *Proc. Natl. Acad. Sci. U.S.A.* **90**, 8342–8346 (1993).
12. A. I. Hernandez, N. Blace, J. F. Crary, P. A. Serrano, M. Leitges, J. M. Libien, G. Weinstein, A. Tcherapanov, T. C. Sacktor, Protein kinase Mζ synthesis from a brain mRNA encoding an independent protein kinase Cζ catalytic domain. Implications for the molecular mechanism of memory. *J. Biol. Chem.* **278**, 40305–40316 (2003).
13. H. Oster, G. Eichele, M. Leitges, Differential expression of atypical PKCs in the adult mouse brain. *Brain Res. Mol. Brain Res.* **127**, 79–88 (2004).
14. A. I. Hernandez, W. C. Oxberry, J. F. Crary, S. S. Mirra, T. C. Sacktor, Cellular and subcellular localization of PKMζ. *Philos. Trans. R. Soc. Lond. B Biol. Sci.* **369**, 20130140 (2014).
15. I. A. Muslimov, V. Nimmrich, A. I. Hernandez, A. Tcherepanov, T. C. Sacktor, H. Tiedge, Dendritic transport and localization of protein kinase Mζ mRNA: Implications for molecular memory consolidation. *J. Biol. Chem.* **279**, 52613–52622 (2004).
16. P. Osten, L. Valsamis, A. Harris, T. C. Sacktor, Protein synthesis-dependent formation of protein kinase Mzeta in long- term potentiation. *J. Neurosci.* **16**, 2444–2451 (1996).
17. P. Tsokas, C. Hsieh, Y. Yao, E. Lesburgueres, E. J. Wallace, A. Tcherepanov, D. Jothianandan, B. R. Hartley, L. Pan, B. Rivard, R. V. Farese, M. P. Sajan, P. J. Bergold, A. I. Hernandez, J. E. Cottrell, H. Z. Shouval, A. A. Fenton, T. C. Sacktor, Compensation for PKMζ in long-term potentiation and spatial long-term memory in mutant mice. *eLife* **5**, e14846 (2016).
18. C. Hsieh, P. Tsokas, P. Serrano, A. I. Hernandez, D. Tian, J. E. Cottrell, H. Z. Shouval, A. A. Fenton, T. C. Sacktor, Persistent increased PKMζ in long-term and remote spatial memory. *Neurobiol. Learn. Mem.* **138**, 135–144 (2017).
19. C. Hsieh, P. Tsokas, A. Grau-Perales, E. Lesburgueres, J. Bukai, K. Khanna, J. Chorny, A. Chung, C. Jou, N. S. Burghardt, C. A. Denny, R. E. Flores-Obando, B. R. Hartley, L. M. Rodriguez Valencia, A. I. Hernandez, P. J. Bergold, J. E. Cottrell, J. M. Alarcon, A. A. Fenton, T. C. Sacktor, Persistent increases of PKMζ in memory-activated neurons trace LTP maintenance during spatial long-term memory storage. *Eur. J. Neurosci.* **54**, 6795–6814 (2021).
20. Y. Hara, M. Punsoni, F. Yuk, C. S. Park, W. G. Janssen, P. R. Rapp, J. H. Morrison, Synaptic distributions of GluA2 and PKMζ in the monkey dentate gyrus and their relationships with aging and memory. *J. Neurosci.* **32**, 7336–7344 (2012).

21. P. P. Gao, J. H. Goodman, T. C. Sacktor, J. T. Francis, Persistent increases of PKMζ in sensorimotor cortex maintain procedural long-term memory storage. *iScience* **5**, 90–98 (2018).
22. L. J. Volk, J. L. Bachman, R. Johnson, Y. Yu, R. L. Huganir, PKM-ζ is not required for hippocampal synaptic plasticity, learning and memory. *Nature* **493**, 420–423 (2013).
23. A. M. Lee, B. R. Kanter, D. Wang, J. P. Lim, M. E. Zou, C. Qiu, T. McMahon, J. Dadgar, S. C. Fischbach-Weiss, R. O. Messing, Prkcz null mice show normal learning and memory. *Nature* **493**, 416–419 (2013).
24. Z. Dong, H. Han, H. Li, Y. Bai, W. Wang, M. Tu, Y. Peng, L. Zhou, W. He, X. Wu, T. Tan, M. Liu, X. Wu, W. Zhou, W. Jin, S. Zhang, T. C. Sacktor, T. Li, W. Song, Y. T. Wang, Long-term potentiation decay and memory loss are mediated by AMPAR endocytosis. *J. Clin. Invest.* **125**, 234–247 (2015).
25. S. Wang, T. Sheng, S. Ren, T. Tian, W. Lu, Distinct roles of PKCι/λ and PKMζ in the initiation and maintenance of hippocampal long-term potentiation and memory. *Cell Rep.* **16**, 1954–1961 (2016).
26. A. Pavlowsky, E. Wallace, A. A. Fenton, J. M. Alarcon, Persistent modifications of hippocampal synaptic function during remote spatial memory. *Neurobiol. Learn. Mem.* **138**, 182–197 (2017).
27. S. F. Palida, M. T. Butko, J. T. Ngo, M. R. Mackey, L. A. Gross, M. H. Ellisman, R. Y. Tsien, PKMζ, but not PKCλ, is rapidly synthesized and degraded at the neuronal synapse. *J. Neurosci.* **35**, 7736–7749 (2015).
28. A. Vogt-Eisele, C. Kruger, K. Duning, D. Weber, R. Spoelgen, C. Pitzer, C. Plaas, G. Eisenhardt, A. Meyer, G. Vogt, M. Krieger, E. Handwerker, D. O. Wennmann, T. Weide, B. V. Skryabin, M. Klugmann, H. Pavenstadt, M. J. Huentelmann, J. Kremerskothen, A. Schneider, KIBRA (KIdney/BRAin protein) regulates learning and memory and stabilizes Protein kinase Mzeta. *J. Neurochem.* **128**, 686–700 (2013).
29. B. L. McNaughton, R. G. M. Morris, Hippocampal synaptic enhancement and information storage within a distributed memory system. *Trends Neurosci.* **10**, 409–415 (1987).
30. E. I. Moser, K. A. Krobert, M. B. Moser, R. G. Morris, Impaired spatial learning after saturation of long-term potentiation. *Science* **281**, 2038–2042 (1998).
31. R. Shema, S. Haramati, S. Ron, S. Hazvi, A. Chen, T. C. Sacktor, Y. Dudai, Enhancement of consolidated long-term memory by overexpression of protein kinase Mzeta in the neocortex. *Science* **331**, 1207–1210 (2011).
32. A. Papassotiropoulos, D. A. Stephan, M. J. Huentelman, F. J. Hoerndli, D. W. Craig, J. V. Pearson, K. D. Huynh, F. Brunner, J. Corneveaux, D. Osborne, M. A. Wollmer, A. Aerni, D. Coluccia, J. Hanggi, C. R. Mondadori, A. Buchmann, E. M. Reiman, R. J. Caselli, K. Henke, D. J. de Quervain, Common Kibra alleles are associated with human memory performance. *Science* **314**, 475–478 (2006).
33. A. Milnik, A. Heck, C. Vogler, H. J. Heinze, D. J. de Quervain, A. Papassotiropoulos, Association of KIBRA with episodic and working memory: A meta-analysis. *Am. J. Med. Genet. B Neuropsychiatr. Genet.* **159B**, 958–969 (2012).
34. K. Buther, C. Plaas, A. Barnekow, J. Kremerskothen, KIBRA is a novel substrate for protein kinase Czeta. *Biochem. Biophys. Res. Commun.* **317**, 703–707 (2004).
35. L. Zhang, S. Yang, D. O. Wennmann, Y. Chen, J. Kremerskothen, J. Dong, KIBRA: In the brain and beyond. *Cell. Signal.* **26**, 1392–1399 (2014).
36. J. Hu, L. Ferguson, K. Adler, C. A. Farah, M. H. Hastings, W. S. Sossin, S. Schacher, Selective erasure of distinct forms of long-term synaptic plasticity underlying different forms of memory in the same postsynaptic neuron. *Curr. Biol.* **27**, 1888–1899.e4 (2017).
37. L. Ferguson, J. Hu, D. Cai, S. Chen, T. W. Dunn, K. Pearce, D. L. Glanzman, S. Schacher, W. S. Sossin, Isoform specificity of PKMs during long-term facilitation in aplysia is mediated through stabilization by KIBRA. *J. Neurosci.* **39**, 8632–8644 (2019).
38. L. Makuch, L. Volk, V. Anggono, R. C. Johnson, Y. Yu, K. Duning, J. Kremerskothen, J. Xia, K. Takamiya, R. L. Huganir, Regulation of AMPA receptor function by the human memory-associated gene KIBRA. *Neuron* **71**, 1022–1029 (2011).
39. F. D. Heitz, M. Farinelli, S. Mohanna, M. Kahn, K. Duning, M. C. Frey, H. Pavenstadt, I. M. Mansuy, The memory gene KIBRA is a bidirectional regulator of synaptic and structural plasticity in the adult brain. *Neurobiol. Learn. Mem.* **135**, 100–114 (2016).
40. M. L. Mendoza, L. D. Quigley, T. Dunham, L. J. Volk, KIBRA regulates activity-induced AMPA receptor expression and synaptic plasticity in an age-dependent manner. *iScience* **25**, 105623 (2022).
41. O. Soderberg, M. Gullberg, M. Jarvius, K. Ridderstrale, K. J. Leuchowius, J. Jarvius, K. Wester, P. Hydbring, F. Bahram, L. G. Larsson, U. Landegren, Direct observation of individual endogenous protein complexes in situ by proximity ligation. *Nat. Methods* **3**, 995–1000 (2006).
42. U. Frey, R. G. Morris, Synaptic tagging and long-term potentiation. *Nature* **385**, 533–536 (1997).
43. E. D. Roberson, J. D. Sweatt, Transient activation of cyclic AMP-dependent protein kinase during hippocampal long-term potentiation. *J. Biol. Chem.* **271**, 30436–30441 (1996).
44. R. Yasuda, Y. Hayashi, J. W. Hell, CaMKII: A central molecular organizer of synaptic plasticity, learning and memory. *Nat. Rev. Neurosci.* **23**, 666–682 (2022).
45. A. Goto, A. Bota, K. Miya, J. Wang, S. Tsukamoto, X. Jiang, D. Hirai, M. Murayama, T. Matsuda, T. J. McHugh, T. Nagai, Y. Hayashi, Stepwise synaptic plasticity events drive the early phase of memory consolidation. *Science* **374**, 857–863 (2021).
46. J. Lisman, Criteria for identifying the molecular basis of the engram (CaMKII, PKMzeta). *Mol. Brain* **10**, 55 (2017).
47. P. Serrano, E. L. Friedman, J. Kenney, S. M. Taubenfeld, J. M. Zimmerman, J. Hanna, C. Alberini, A. E. Kelley, S. Maren, J. W. Rudy, J. C. Yin, T. C. Sacktor, A. A. Fenton, PKMzeta maintains spatial, instrumental, and classically conditioned long-term memories. *PLoS Biol.* **6**, 2698–2706 (2008).
48. J. L. Kwapis, T. J. Jarome, M. E. Lonergan, F. J. Helmstetter, Protein kinase Mzeta maintains fear memory in the amygdala but not in the hippocampus. *Behav. Neurosci.* **123**, 844–850 (2009).
49. K. Si, E. R. Kandel, The role of functional prion-like proteins in the persistence of memory. *Cold Spring Harb. Perspect. Biol.* **8**, a021774 (2016).
50. R. Y. Tsien, Very long-term memories may be stored in the pattern of holes in the perineuronal net. *Proc. Natl. Acad. Sci. U.S.A.* **110**, 12456–12461 (2013).
51. S. Heo, G. H. Diering, C. H. Na, R. S. Nirujogi, J. L. Bachman, A. Pandey, R. L. Huganir, Identification of long-lived synaptic proteins by proteomic analysis of synaptosome protein turnover. *Proc. Natl. Acad. Sci. U.S.A.* **115**, E3827–E3836 (2018).
52. P. Shrestha, E. Klann, Spatiotemporally resolved protein synthesis as a molecular framework for memory consolidation. *Trends Neurosci.* **45**, 297–311 (2022).
53. Y. Yao, M. T. Kelly, S. Sajikumar, P. Serrano, D. Tian, P. J. Bergold, J. U. Frey, T. C. Sacktor, PKMζ maintains late long-term potentiation by N-ethylmaleimide-sensitive factor/GluR2-dependent trafficking of postsynaptic AMPA receptors. *J. Neurosci.* **28**, 7820–7827 (2008).
54. J. G. Hanley, L. Khatri, P. I. Hanson, E. B. Ziff, NSF ATPase and alpha-/beta-SNAPs disassemble the AMPA receptor-PICK1 complex. *Neuron* **34**, 53–67 (2002).
55. P. V. Migues, O. Hardt, D. C. Wu, K. Gamache, T. C. Sacktor, Y. T. Wang, K. Nader, PKMζ maintains memories by regulating GluR2-dependent AMPA receptor trafficking. *Nat. Neurosci.* **13**, 630–634 (2010).
56. D. O. Wennmann, J. Schmitz, M. C. Wehr, M. P. Krahn, N. Koschmal, S. Gromnitza, U. Schulze, T. Weide, A. Chekuri, B. V. Skryabin, V. Gerke, H. Pavenstadt, K. Duning, J. Kremerskothen, Evolutionary and molecular facts link the WWC protein family to Hippo signaling. *Mol. Biol. Evol.* **31**, 1710–1723 (2014).
57. N. Otmakhov, L. C. Griffith, J. E. Lisman, Postsynaptic inhibitors of calcium/calmodulin-dependent protein kinase type II block induction but not maintenance of pairing-induced long-term potentiation. *J. Neurosci.* **17**, 5357–5365 (1997).
58. I. Buard, S. J. Coultrap, R. K. Freund, Y. S. Lee, M. L. Dell'Acqua, A. J. Silva, K. U. Bayer, CaMKII "autonomy" is required for initiating but not for maintaining neuronal long-term information storage. *J. Neurosci.* **30**, 8214–8220 (2010).
59. H. Murakoshi, M. E. Shin, P. Parra-Bueno, E. M. Szatmari, A. C. Shibata, R. Yasuda, Kinetics of endogenous CaMKII required for synaptic plasticity revealed by optogenetic kinase inhibitor. *Neuron* **94**, 37–47.e5 (2017).
60. W. Tao, J. Lee, X. Chen, J. Diaz-Alonso, J. Zhou, S. Pleasure, R. A. Nicoll, Synaptic memory requires CaMKII. *Elife* **10**, e60360 (2021).
61. J. H. Choi, S. E. Sim, J. I. Kim, D. I. Choi, J. Oh, S. Ye, J. Lee, T. Kim, H. G. Ko, C. S. Lim, B. K. Kaang, Interregional synaptic maps among engram cells underlie memory formation. *Science* **360**, 430–435 (2018).
62. T. J. Ryan, D. S. Roy, M. Pignatelli, A. Arons, S. Tonegawa, Memory., Engram cells retain memory under retrograde amnesia. *Science* **348**, 1007–1013 (2015).
63. W. Aziz, I. Kraev, K. Mizuno, A. Kirby, T. Fang, H. Rupawala, K. Kasbi, S. Rothe, F. Jozsa, K. Rosenblum, M. G. Stewart, K. P. Giese, Multi-input synapses, but not LTP-strengthened synapses, correlate with hippocampal memory storage in aged mice. *Curr. Biol.* **29**, 3600–3610.e4 (2019).
64. W. C. Abraham, O. D. Jones, D. L. Glanzman, Is plasticity of synapses the mechanism of long-term memory storage? *NPJ Sci. Learn.* **4**, 9 (2019).
65. A. I. Ramsaran, Y. Wang, A. Golbabaei, S. Aleshin, M. L. de Snoo, B. A. Yeung, A. J. Rashid, A. Awasthi, J. Lau, L. M. Tran, S. Y. Ko, A. Abegg, L. C. Duan, C. McKenzie, J. Gallucci, M. Ahmed, R. Kaushik, A. Dityatev, S. A. Josselyn, P. W. Frankland, A shift in the mechanisms controlling hippocampal engram formation during brain maturation. *Science* **380**, 543–551 (2023).
66. G. Kauwe, K. A. Pareja-Navarro, L. Yao, J. H. Chen, I. Wong, R. Saloner, H. Cifuentes, A. L. Nana, S. Shah, Y. Li, D. Le, S. Spina, L. T. Grinberg, W. W. Seeley, J. H. Kramer, T. C. Sacktor, B. Schilling, L. Gan, K. B. Casaletto, T. E. Tracy, KIBRA repairs synaptic plasticity and promotes resilience to tauopathy-related memory loss. *J. Clin. Invest.* **134**, (2024).
67. I. J. Cajigas, G. Tushev, T. J. Will, S. T. Dieck, N. Fuerst, E. M. Schuman, The local transcriptome in the synaptic neuropil revealed by deep sequencing and high-resolution imaging. *Neuron* **74**, 453–466 (2012).
68. M. T. Kelly, J. F. Crary, T. C. Sacktor, Regulation of protein kinase Mζ synthesis by multiple kinases in long-term potentiation. *J. Neurosci.* **27**, 3439–3444 (2007).
69. P. R. Westmark, C. J. Westmark, S. Wang, J. Levenson, K. J. O'Riordan, C. Burger, J. S. Malter, Pin1 and PKMzeta sequentially control dendritic protein synthesis. *Sci. Signal.* **3**, ra18 (2010).
70. R. L. Redondo, R. G. Morris, Making memories last: The synaptic tagging and capture hypothesis. *Nat. Rev. Neurosci.* **12**, 17–30 (2011).

71. Y. Kodama, C. D. Hu, Bimolecular fluorescence complementation (BiFC): A 5-year update and future perspectives. *Biotechniques* **53**, 285–298 (2012).
72. Plutarch, Theseus in *Lives, Volume I: Theseus and Romulus. Lycurgus and Numa. Solon and Publicola*, Loeb Classical Library, B. Perrin, Transl. (Harvard University Press, 1914), chap. 23.1.
73. P. Tsokas, B. Rivard, C. Hsieh, J. E. Cottrell, A. A. Fenton, T. C. Sacktor, Antisense oligodeoxynucleotide perfusion blocks gene expression of synaptic plasticity-related proteins without inducing compensation in hippocampal slices. *Bio Protoc.* **9**, e3387 (2019).
74. P. Tsokas, E. A. Grace, P. Chan, T. Ma, S. C. Sealfon, R. Iyengar, E. M. Landau, R. D. Blitzer, Local protein synthesis mediates a rapid increase in dendritic elongation factor 1A after induction of late long-term potentiation. *J. Neurosci.* **25**, 5833–5843 (2005).
75. W. W. Anderson, G. L. Collingridge, Capabilities of the WinLTP data acquisition program extending beyond basic LTP experimental functions. *J. Neurosci. Methods* **162**, 346–356 (2007).
76. T. Peng, K. Thorn, T. Schroeder, L. Wang, F. J. Theis, C. Marr, N. Navab, A BaSiC tool for background and shading correction of optical microscopy images. *Nat. Commun.* **8**, 14836 (2017).
77. T. D. Goddard, C. C. Huang, E. C. Meng, E. F. Pettersen, G. S. Couch, J. H. Morris, T. E. Ferrin, UCSF ChimeraX: Meeting modern challenges in visualization and analysis. *Protein Sci.* **27**, 14–25 (2018).
78. E. F. Pettersen, T. D. Goddard, C. C. Huang, E. C. Meng, G. S. Couch, T. I. Croll, J. H. Morris, T. E. Ferrin, UCSF ChimeraX: Structure visualization for researchers, educators, and developers. *Protein Sci.* **30**, 70–82 (2021).
79. U. Pieper, N. Eswar, H. Braberg, M. S. Madhusudhan, F. P. Davis, A. C. Stuart, N. Mirkovic, A. Rossi, M. A. Marti-Renom, A. Fiser, B. Webb, D. Greenblatt, C. C. Huang, T. E. Ferrin, A. Sali, MODBASE, a database of annotated comparative protein structure models, and associated resources. *Nucleic Acids Res.* **32**, 217D–2222D (2004).
80. C. A. Schneider, W. S. Rasband, K. W. Eliceiri, NIH Image to ImageJ: 25 years of image analysis. *Nat. Methods* **9**, 671–675 (2012).
81. A. M. Delachat, N. Guidotti, A. L. Bachmann, A. C. A. Meireles-Filho, H. Pick, C. C. Lechner, C. Deluz, B. Deplancke, D. M. Suter, B. Fierz, Engineered multivalent sensors to detect coexisting histone modifications in living stem cells. *Cell Chem. Biol.* **25**, 51–56 e56 (2018).
82. A. Garcia-Osta, P. Tsokas, G. Pollonini, E. M. Landau, R. Blitzer, C. M. Alberini, MuSK expressed in the brain mediates cholinergic responses, synaptic plasticity, and memory formation. *J. Neurosci.* **26**, 7919–7932 (2006).
83. E. M. M. Manders, F. J. Verbeek, J. A. Aten, Measurement of co-localization of objects in dual-colour confocal images. *J. Microsc.* **169**, 375–382 (1993).

Acknowledgments: P.T. is an Alexander S. Onassis Public Benefit Foundation Scholar. **Funding:** This work was supported by the National Institutes of Health [grant R37 MH057068 (T.C.S.)], National Institutes of Health [grant R01 MH115304 (T.C.S. and A.A.F.)], National Institutes of Health [grant R01 NS105472 (A.A.F.)], National Institutes of Health [grant R01 MH132204 (A.A.F.)], National Institutes of Health [grant R01 NS108190 (P.J.B. and T.C.S.)], Natural Sciences and Engineering Research Council of Canada Discovery [grant 203523 (K.N.)], and the Garry & Sarah S. Sklar Fund (P.T.). **Author contributions:** Conceptualization: T.C.S., A.A.F., K.N., H.Z.S., P.T., C.H., R.E.F.-O., A.I.H., M.B., J.E.C., J.K., and A.T. Methodology: P.T., C.H., R.E.F.-O., A.T., A.I.H., M.B., K.N., A.A.F., and T.C.S. Investigation: P.T., C.H., R.E.F.-O., M.B., A.T., J.K., C.T., and T.C.S. Project administration: T.C.S., A.A.F., and P.T. Resources: P.T., C.H., A.T., J.E.C., J.K., K.N., A.A.F., and T.C.S. Data curation: C.H., P.T., R.E.F.-O., and A.T. Validation: P.T., C.H., R.E.F.-O., M.B., A.T., J.K., A.A.F., and T.C.S. Supervision: T.C.S., A.A.F., P.T., K.N., A.I.H., and J.E.C. Software: A.A.F. Visualization: C.H., P.T., A.I.H., and T.C.S. Formal analysis: C.H., P.T., R.E.F.-O., A.A.F., and T.C.S. Writing—original draft: T.C.S. Writing—reviewing and editing: A.A.F., T.C.S., K.N., P.J.B., H.Z.S., P.T., C.H., R.E.F.-O., M.B., A.T., A.I.H., C.T., J.E.C., and J.K. Funding acquisition: T.C.S., A.A.F., P.J.B., K.N., and J.E.C. **Competing interests:** T.C.S. is an inventor on a patent application (serial number 63/597,518) submitted by The Research Foundation for The State University of New York on 11/9/2023, pertaining to results presented in the paper. The other authors declare that they have no competing interests. **Data and materials availability:** All data needed to evaluate the conclusions in the paper are present in the paper and/or the Supplementary Materials. Requests for plasmids, antisera, and other materials used in this study may be made to T.C.S.

Submitted 22 September 2023
Accepted 23 May 2024
Published 26 June 2024
10.1126/sciadv.adl0030